Some like it hot: efficiency of the type III secretion system and activation of plant defenses have multiple thermosensitive behaviors in the *Pseudomonas syringae* complex

E. Caullireau[1,2], D. Danzi[1], V.M. Tempo[1], M. Pandolfo[1], C.E. Morris[2], E. Vandelle[1*]

[1] Department of Biotechnology, University of Verona, Verona, Italy.

[2] UR0407 Plant Pathology, INRAE, Montfavet, France.

*Corresponding author:

Email: elodiegenevieve.vandelle@univr.it (EV)

Abstract

The *Pseudomonas syringae* species complex is a very important plant pathogenic bacterium, causing damage and economic losses on many crops. Research efforts for the understanding of the determinants of the host-range of a given strain are considerable. Recently, we showed that the inability of a *P. syringae* pv. *actinidiae* strain to trigger ETI in *A. thaliana* is due to an inefficient T3SS and not to the absence of a recognized effector. In this context, we compared several *P. syringae* strains belonging to different phylogroups and carrying the same plasmid-born avirulence gene for their ability to induce an HR in *A. thaliana* Col-0, as a marker of T3SS efficiency.

Pto DC3000 *AvrB* and *Pma* M6 *AvrB* consistently triggered a strong HR while other strains induced it at different intensities significantly depending on temperature. Both behaviors of low and warm temperature-dependency for T3SS efficiency were observed among thermosensitive strains, irrespective of their *in-vitro* growth optimum. Surprisingly, differences were also observed among quasi-clonal strains. These results reveal a strongly strain-specific regulatory role of temperature in effector injection and reinforce the notion that the presence/absence of effectors is not sufficient to predict the outcome of plant-bacteria interactions. Moreover, this work highlights the necessity to study bacterial virulence in a broader set of strains insofar as *Pto* DC3000 is a reliable model strain but not representative of the *P. syringae* complex.

Author summary

Pseudomonas syringae is a bacterium ubiquitous in the environment and responsible for important crop losses worldwide. Moreover, *P. syringae* serves as a model organism for studying plant-pathogen interactions. Bacteria rely on various virulence mechanisms to successfully infect their host, one of the most important of which is the Type III Secretion System (T3SS). Although it is acknowledged that environmental conditions play a significant role in the plant-pathogen interactions, our understanding of their influence on both partners is still limited. Regarding temperature, contrasting findings have been reported about its influence on T3SS efficiency. While most efforts have focused on a few strains of *P. syringae*, the phylogenetic diversity of this bacterium is enormous. Consequently, we decided to characterize the role of temperature on T3SS efficiency in *P. syringae* in a broader way. Our results showed that bacterial behavior in response to temperature is highly variable among strains, even among very closely related ones. Our study

43 provides new insights into the role of temperature in regulating bacterial virulence and further
44 evidence of the need to investigate the diversity of pathogenic organisms beyond model strains.
45

46 Introduction

47 *Pseudomonas syringae* is a gram-negative bacterium that poses a threat to global agricultural
48 production with new outbreaks that emerge regularly [1,2]. *P. syringae* has been divided into 13
49 phylogenetic groups (phylogroups, PG), further divided into 23 clades [3]. During the infection
50 process, *P. syringae* relies on an arsenal of secreted virulence factors, such as secretion systems,
51 quorum sensing (QS), production of phytotoxins (coronatine, syringomycin…), hormones,
52 exopolysaccharides (EPS), siderophores etc. [4,5]. *P. syringae* pathogenesis is predominantly
53 mediated by the type III secretion system (T3SS), a highly conserved needle-like specialized
54 protein secretion machinery, found in numerous gram-negative bacterial pathogens affecting
55 plants and animals. T3SS forms a continuous channel, guiding the translocation of diverse
56 proteinaceous effectors (T3SEs) from the bacterium directly into the host cell or apoplast [6–9].
57 T3SEs facilitate the invasion of plant host cells, suppress plant immunity, or interfere with essential
58 plant cellular processes [10–15]. *P. syringae* strains in the phylogroups with the canonical T3SS
59 commonly harbor a repertoire of approximately 15-30 T3SEs, playing distinct roles within the host
60 plant [16–21]. Of note, there is no direct relationship between the size or content of the T3SE
61 repertoire and host range [22,23]. When considered individually, numerous T3SEs are dispensable
62 for *P. syringae* virulence. However, collectively, they redundantly contribute to disarming plant
63 immunity [19,24].

64 Throughout their co-evolution with pathogens, plants have evolved an extensive array of defenses
65 to recognize them and block pathogenesis. Common bacterial features such as flagellin,
66 lipopolysaccharide (LPS), peptidoglycan and elongation factor Tu (EF-Tu) contain conserved
67 molecular motifs (Pathogen or Microbe-Associated Molecular Patterns; P/MAMPs) that are
68 sensed by the plant as non-self, through their binding to Pattern Recognition Receptors (PRRs)
69 situated on the plant cell surface [25,26]. Non-self detection by PRRs is the first step of the PTI or
70 MTI, for PAMP-/MAMP-Triggered Immunity, implying then various cellular responses to inhibit
71 pathogen growth and virulence mechanisms, such as T3SS activation for bacterial pathogens
72 [27,28]. On the other hand, T3SEs serve the primary function of subverting PTI, targeting key
73 signaling components to interfere with their function. In response, plants have evolved
74 cytoplasmic receptors called 'resistance' (R) proteins to detect some of these effectors, either
75 directly or indirectly, leading to the activation of the Effector-Triggered Immunity (ETI) [29]. R
76 genes typically encode for NLR proteins (Nucleotide-binding oligomerization domain-Like
77 Receptor), consisting of a nucleotide-binding site (NBS) and a leucine-rich repeat (LRR) domain
78 [30]. PTI and ETI are unlikely to be separate processes as suggested in the 'zigzag' model [31], but
79 both non-self and virulence effector recognition by membrane and cytoplasmic receptors are
80 simultaneously involved in a global surveillance system to respond effectively to pathogen attack
81 [32,33]. ETI is a potentiation of PTI, often leading to rapid and localized programmed cell death,
82 known as the hypersensitive response (HR). HR generally occurs within 2 to 6 hours post initial
83 host-pathogen contact, inhibiting the propagation of (hemi)-biotrophic pathogens, such as *P.*
84 *syringae* [34,35].

85 According to the 'disease triangle' paradigm [36], plant diseases arise from the interplay between
86 a susceptible plant and a virulent pathogen, under conducive environmental conditions, resulting
87 in a compatible reaction. Overall plant-pathogen interaction mechanisms are highly influenced by
88 environmental conditions, which can either favor, have neutral effects, or hinder both partners
89 [21,37]. Among the environmental factors, temperature has a regulatory role of virulence in plant-
90 associated bacteria (reviewed in references [37,38]).
91 Within the *P. syringae* species complex, temperature variations impact various traits crucial for
92 bacterial fitness, including phytotoxins, EPS biosynthesis, motility or quorum-sensing [38–52].
93 T3SS has also been investigated concerning its possible thermoregulation. In *P. syringae* pv.
94 *syringae* and pv. *tomato* DC3000, the *in-vitro* secretion of HopPsyA and AvrPto effectors was
95 impaired at temperatures above 22°C and 20°C, indicating some kind of low-temperature
96 dependency for their T3SS efficiency [53]. In contrast, recent findings in strain DC3000 revealed
97 that the translocation of T3SEs in *A. thaliana* cells is enhanced at 30°C compared to 23°C,
98 indicating the possible T3SS efficiency even at elevated temperatures [54]. However, in tomato,
99 the expression of T3SS-related genes *hrpL* and *hrpA* in this same strain was not affected by a
100 temperature rise from 26°C to 31°C, although the expression of the avirulence gene *AvrPtoB* was
101 significantly reduced [48]. On the other hand, for *P. syringae* pv. *actinidiae* strains, it was shown
102 that there was no difference in *hrpA1* promoter activity *in vitro* across a temperature range of 18-
103 28°C, nonetheless, substantial differences were evident at a functional level, demonstrating a low-
104 temperature dependency for T3SS efficiency for these strains [55]. However, the complete
105 implications of warm temperatures on *P. syringae* virulence in plants remain poorly understood
106 [39,47]. Studies indicate complex interactions with plant immune signaling pathways,

107 emphasizing the need for further research to understand their implications in terms of disease
108 [54,56].
109 Thermosensing principles in phytopathogens are less understood than those of pathogens of
110 warm-blooded organisms. They were assumed to be different, given the ecological differences
111 between these groups of pathogens [38,57]. Nevertheless, some common mechanisms have been
112 identified in both plant- and mammal-associated bacteria. Various molecular strategies are
113 involved in sensing temperature, such as two-component systems (TCSs) that typically involve a
114 membrane-bound sensor histidine kinase that detects environmental stimuli and a cytoplasmic
115 response regulator influencing gene expression upon phosphorylation of an aspartic acid [57].
116 Several TCS were shown to be involved in the thermoregulation of virulence mechanisms, such as
117 the VirA/G system in *Agrobacterium tumefaciens* [58], the GacS/GacA system in *P. syringae* pv.
118 *phaseolicola* [59,60] and the CorRSP system in *P. syringae* pv. *glycinea* [61].
119 Evidence of the influence of temperature in regulating virulence factors in *P. syringae* species
120 complex has been documented, however, there have not been studies dedicated to comparing
121 strains under identical conditions. Consequently, we wanted to further understand the role of the
122 temperature on the function/activation dynamics of the T3SS, investigating a broader range of
123 diversity within the *P. syringae* species complex under comparable conditions. For this purpose,
124 we transformed 13 strains of *P. syringae* to carry the effector AvrB and infiltrated them into
125 *Arabidopsis thaliana* Col-0 leaf disks. In this model plant, AvrB is indirectly recognized by the
126 resistance protein RPM1, through RIN4 modification, which triggers HR [62–64]. Infiltrated leaf
127 disks were incubated at different temperatures and the quantification of electrolyte leakage
128 served as the indicator of HR onset. Conductivity increase was used as a proxy for T3SS efficiency,

129 and this allowed us to effectively discriminate strains based on a robust phenotype directly linked
130 to the activation of the T3SS. Based on the different behaviors we observed in response to
131 temperature, we investigated the genomes of the strains in an attempt to decipher the origin of
132 the thermosensing mechanisms.
133

134 Results

135 The intensity of HR induction is not strictly reproducible for individual 136 strains.

137 To evaluate T3SS functionality at different temperatures, *AvrB*-expressing *P. syringae* strains were
138 infiltrated into *A. thaliana* Col-0 leaf disks. As a T3SS-dependent mechanism, HR was quantified
139 by measuring the increase in ion leakage due to dying cells. Conductivity levels measured among
140 the diverse replicated experiments were highly variable. The conductivity value measured at 24
141 hours post-infection (hpi) for a given modality (*i.e.*, one strain infiltrated and incubated at one
142 temperature) doubled or tripled among replicated experiments (*e.g*. conductivity values ranged
143 from 80 $\mu S.cm^{-1}$ to 226 $\mu S.cm^{-1}$ for strain DC3000 *AvrB* when incubated at 18°C) (Fig 1). This
144 variability is illustrated in Fig 2 for the seven replicated experiments for strain USA007 *AvrB* at 18°C
145 (ratio of areas under the curves calculated for the replicated experiments that induced the most
146 and the least = 2.8). Moreover, conductivity showed considerable heteroscedasticity, *i.e.* there
147 was a positive correlation between the mean area under the curves and their variance with
148 Spearman's coefficient = 0.91; $p < 0.05$ (S1 Fig). Four examples of the relationship between

149 variability and mean conductivity are shown in Fig 2. This large variability raised the question of
150 how the HR induction could be quantified to compare the strains, as addressed in the next section.
151
152 **Fig 1. Variability in the increase of conductivity measured at 24 hours post-inoculation (hpi) over**
153 **the replicated experiments performed for each *AvrB*-expressing strain, at 18°C (A), 24°C (B) and**
154 **28°C (C).** Bars represent the mean increase in conductivity for each of the independent biological
155 replicates ($3 \leq n \leq 27$). Values are sorted from left to right in a descending order.
156
157 **Fig 2. Electrolyte leakage curves obtained post-infiltration for strain M6 *AvrB* at 18°C (A), USA007**
158 ***AvrB* at 18°C (B), LAB0041 *AvrB* at 24°C (C) and CC1498 *AvrB* at 28°C (D).** Each curve represents
159 the mean increase in conductivity measured over time for one independent biological replicate
160 performed with three technical replicates each. Error bars represent standard error.
161

162 Intensity of HR induction varies among strains.

163 To compare HR induction intensity among strains, we accounted for the variability described
164 above by fitting Linear Mixed effects Models to our data. This statistical approach allowed us to
165 classify strains as inducers or non-inducers at each of the temperatures that we tested. This
166 revealed that almost all the *P. syringae* strains induced HR except for J35 *AvrB* at all the
167 temperatures, MAFF302273 *AvrB* at 24°C and 28°C, B728a *AvrB* at 24°C, and 1448A and CRA-FRU
168 8.43 at 28°C (Table 1). The inducer strains led to conductivity levels that were significantly greater
169 than those measured in the mock treatment (10mM $MgCl_2$ or *hrp*-inducing medium HIM) ($p <$
170 0.05) according to Linear Mixed-effects Models. More specifically, our results demonstrated that

171 all the inducer strains varied in the intensity of the HR induction they caused. The model estimated
172 the mean difference in points of conductivity measured between the tested modality and the
173 mock treatment. The values presented in Table 1 ("Estimate") are proxies of the intensity of HR
174 induction for each strain. DC3000 *AvrB* and M6 *AvrB* displayed the highest values ("Estimate" > 65
175 regardless of the temperature tested), whereas some others such as the three quasi-clonal strains
176 CC0073 *AvrB*, CC0094 *AvrB* and CC1498 *AvrB* averaged less than 20. These differences are also
177 reflected in the mean areas under conductivity progress curves (AUCPC) at each temperature as
178 shown in Fig 3. This proxy of the HR induction intensity was correlated neither with the *AvrB*
179 expression levels (S2 Fig) nor with the bacterial growth capacity at a given temperature (S3 Fig).
180

181 **Table 1. Statistics associated with linear mixed-effects models fitted to ion leakage experiment**
182 **results.**

PHYLOGROUP	STRAIN	INDUCER AT A GIVEN TEMPERATURE						TEMPERATURE	
		18°C		24°C		28°C			
		Estimate	*p-value*	*Estimate*	*p-value*	*Estimate*	*p-value*	*p-value*	*Estimate*
1a	DC3000	69.97	**2.00E-16**	73.12	**1.25E-15**	65.27	**8.46E-15**	8.02E-01	-0.19
	M6	95.14	**2.00E-16**	89.06	**5.35E-16**	73.05	**1.59E-14**	1.95E-01	-2.07
	T1	28.98	**2.00E-16**	29.07	**2.00E-16**	13.45	**2.81E-08**	**1.42E-02**	**-1.26**
	LAB0041	31.36	**4.24E-11**	29.56	**2.00E-16**	16.83	**2.83E-09**	5.17E-02	-1.22
1b	J35	3.35	5.43E-02	0.18	9.19E-01	-1.27	4.46E-01	NA	
	CRA-FRU 8.43	14.09	**4.69E-11**	4.97	**4.33E-04**	0.97	4.45E-01	**3.80E-03**	**-1.28**
	USA007	52.24	**2.00E-16**	46.69	**8.58E-16**	34.15	**2.26E-12**	**3.35E-02**	**-1.70**
2d	CC0073	15.22	**5.97E-07**	15.28	**7.62E-07**	19.77	**3.42E-09**	3.55E-01	0.63
	CC0094	6.86	**6.44E-08**	9.72	**2.61E-06**	14.49	**8.91E-08**	**9.76E-04**	**0.97**
	CC1498	7.89	**4.96E-06**	12.69	**2.24E-05**	19.96	**1.52E-08**	**2.58E-02**	**1.36**
	B728a	3.12	**2.08E-02**	2.22	1.61E-01	4.75	**8.07E-03**	**4.27E-02**	**0.37**
	MAFF302273	3.17	**1.73E-02**	2.88	9.68E-02	1.78	3.77E-01	NA	
3a	1448A	5.14	**1.07E-02**	6.73	**9.73E-03**	2.46	2.41E-01	6.41E-01	0.53

183 The effect of strains was calculated for each mutant bacterium at each temperature by comparing
184 with the results obtained for the mock treatment (10mM $MgCl_2$). Significant values of the estimate
185 parameter ($p < 0.05$, in bold) are associated with HR inducing conditions. The temperature effect
186 was evaluated for each *AvrB*-expressing strain, inducing HR at least at two temperatures (non-
187 inducer strains are highlighted in grey), comparing the electrolyte leakage curves obtained at
188 these different temperatures. Strains insensitive to the temperature ($p > 0.05$) are highlighted in
189 green, strains leading to minor conductivity levels as the temperature increases (negative
190 estimate, $p < 0.05$) are highlighted in blue, and strains displaying a warm-dependency (positive
191 estimate, $p < 0.05$) are highlighted in red. The number of replicated experiments for each modality
192 (strain x temperature condition) varied from 3 up to 27.
193
194 **Fig 3. Mean area under conductivity progress curve (AUCPC) calculations for all the replicated**
195 **experiments ($3 \leq n \leq 27$) of each *AvrB*-expressing strain at 18°C (A), 24°C (B) and 28°C (C).** Error
196 bars represent standard error.
197

198 Intensity of HR induction is temperature-sensitive in half of the inducer
199 strains.

200 With Linear Mixed-effects Models, we categorized the HR inducer strains according to the
201 temperature-sensitivity of HR induction. Six out of eleven strains were insensitive to a change in
202 temperature (DC3000 *AvrB*, M6 *AvrB*, LAB0041 *AvrB*, CC0073 *AvrB*, 1448A *AvrB*) ($p > 0.05$) (Table
203 1). The other HR inducer strains were considered temperature-sensitive ($p < 0.05$) and could be
204 categorized into two groups according to whether the "Estimate" values were negative or positive.

205 In one group, strains showed higher conductivity with lower temperatures (T1 *AvrB*, CRA-FRU 8.43
206 *AvrB* and USA007 *AvrB*). In the case of CRA-FRU 8.43 *AvrB* strain, the decrease in conductivity
207 observed with increasing temperature led the strain to be categorized as a non-inducer at 28°C
208 (Table 1). In the other group, strains showed higher conductivity with higher temperatures
209 (CC0094 *AvrB*, CC1498 *AvrB* and B728a *AvrB*). Temperature-sensitivity of the *AvrB*-expressing
210 strains was further confirmed by the analysis of HrpZ secretion *in vitro* as an assessment of T3SS
211 functionality. Interestingly, the strain MAFF302273 *AvrB* displayed a functional T3SS, while it
212 constantly did not lead to conductivity increase once infiltrated into leaf disks, suggesting T3SS
213 inactivation in *A. thaliana* (S4 Fig).
214

215 Temperature responsiveness patterns vary among strains but remain
216 consistent within the same phylogroup.

217 A given phylogroup could contain strains that induced HR in temperature-sensitive and
218 temperature-insensitive ways (Table 1). However, temperature-sensitive strains within a same
219 phylogroup showed the same trend relative to increasing temperature. Indeed, the group of
220 strains whose T3SS was more efficient at the cooler temperatures (*i.e.*, low-temperature-
221 dependent; T1 *AvrB*, CRA-FRU 8.43 *AvrB* and USA007 *AvrB*) and the group whose T3SS was more
222 efficient at warmer temperatures (*i.e.*, warm-temperature-dependent; CC0094 *AvrB*, CC1498 *AvrB*
223 and B728a *AvrB*) belong to the phylogroups 1 and 2d, respectively (Table 1). Additionally, HrpZ
224 secretion by MAFF302273 *AvrB* was more important as the temperature rose, revealing a pattern
225 of warm-temperature dependency for T3SS efficiency, similar to the other thermosensitive strains
226 belonging to the same phylogroup 2d (S4 Fig). Nevertheless, dramatic differences among strains

227 even very closely related phylogenetically were still observed, as illustrated by the three quasi-
228 clonal *AvrB*-expressing strains from phylogroup 2d, CC0073, CC0094 and CC1498 (Table 1) (Fig 4).
229 CC0073 *AvrB* was temperature-independent in its ability to induce HR while CC0094 *AvrB* and
230 CC1498 *AvrB* both showed clearly greater capacity at warmer temperatures. Moreover, in terms
231 of intensity, CC1498 *AvrB* led to higher values of conductivity measured at 24 hpi than CC0073
232 *AvrB* and CC0094 *AvrB*. Finally, in terms of kinetics, CC0073 *AvrB* was responsible for a faster HR
233 induction at the beginning of the interaction – no matter the temperature concerned – that
234 stalled, whereas CC0094 *AvrB* and CC1498 *AvrB* were much slower in inducing HR (Fig 4).
235
236 **Fig 4. Electrolyte leakage curves over time obtained post-infiltration for CC0073 *AvrB* (A),**
237 **CC0094 *AvrB* (B) and CC1498 *AvrB* (C).** Infiltrated leaf disks were incubated at 18°C (blue), 24°C
238 (pink) and 28°C (red). Conductivity following infiltration of the mock treatment (10mM $MgCl_2$) and
239 incubation at 24°C is represented by the black dotted line. Data represent one single
240 representative biological replicate with all strains and temperature conditions evaluated
241 simultaneously with three technical replicates each. Error bars represent standard error.
242

243 Strains from the *P. syringae* complex display diverse speeds of HR
244 induction.

245 To account for dynamic aspects in the behaviors of *AvrB*-expressing *P. syringae* strains, the ratio
246 of conductivity values measured at 6 hpi and 24 hpi was calculated for each replicated experiment
247 for all modalities that were found to be HR-inducing. This parameter was used as a proxy for HR
248 induction velocity. An analysis of variance of these ratios revealed significant differences among

249 *AvrB*-expressing strains (ANOVA1, $p < 0.05$). DC3000 *AvrB* and M6 *AvrB* proved to be the fastest
250 HR inducers with more than 70% of their total induction already observable at 6 hpi (Fig 5). Yet
251 again, the diversity of behaviors within phylogroups was revealed, even among the three *AvrB*-
252 expressing quasi-clonal strains (Fig 5, post-hoc Dunn's test showed that CC0073 *AvrB* and CC0094
253 *AvrB* and CC1498 *AvrB* groups differed significantly at $p < 0.05$). Furthermore, 6 hpi/24 hpi-ratios
254 were compared across the different temperatures overall revealing that higher temperatures
255 correlated with faster electrolyte leakage, consistent with the results observed for bacterial *in-*
256 *vitro* growth (S5 Fig).
257
258 **Fig 5**. **Estimation of velocity of HR induction.** The proxy for velocity was calculated as the ratio of
259 conductivity increase measured at 6 hpi and 24 hpi for each *AvrB*-expressing strain inducing HR at
260 least at one temperature condition. Strains are sorted by phylogroup from left to right, PG1a
261 (purple), PG1b (green), PG2d (yellow), PG3a (red). Boxes were calculated from 5 up to 73
262 replicated experiments per strain (single dots). Boxes associated with different letters represent
263 significantly different means ($p < 0.05$, according to a Kruskal-Wallis's test followed by post-hoc
264 Dunn's test).
265

266 Whole genome sequences suggest a few candidate genes for
267 temperature-sensitivity.

268 As we wanted to decipher the origin of sensitivity to the temperature for HR induction, we applied
269 a comparative genomic approach focusing on the three quasi-clonal strains CC0073, CC0094 and
270 CC1498. These strains displayed at least 99.84% homology (ANI calculation). Among the whole set

271 of strains, 286 putative genes were specific to the three CC-strains, and 76 were common only to
272 the two warm temperature-dependent ones (CC0094 and CC1498) (Fig 6). By comparing the
273 putative genes present in CC0094 and CC1498 but missing in CC0073 (regardless of their
274 presence/absence in the other strains) the list was extended to 173 genes, with 94% of the
275 proteins encoded by these genes unknown (neither the name nor the function) and only 10
276 putative genes with a known or putative function (S1 Table).
277
278 **Fig 6. Comparative genomics performed for the 13 strains characterized in ion leakage**
279 **experiments.** Vertical bars correspond to the number of genes shared by groups of strains or
280 exclusively present in single strains (group/strain-specific genes). Horizontal color bars represent
281 the type of behavior of each strain in response to temperature, as identified in Table 1. Common
282 putative genes specific to the 3 quasi-clonal strains CC0073, CC0094 and CC1498 are in yellow,
283 common putative genes specific to CC0094 and CC1498 are in red.
284

285 # Discussion

286 ## New perspectives on virulence thermoregulation processes.

287 The diverse behaviors of T3SS efficiency observed in relation to incubation temperature indicate
288 that temperature plays a crucial role in regulating bacterial virulence. This observation is another
289 piece of evidence out of the many reported over the past 30 years regarding the role of
290 temperature in virulence regulation in plant-associated bacteria (reviewed in references [37,38]).
291 Our work has presented new examples of relatively warm-temperature dependency for virulence

292 efficiency, consistent with previous findings about gene expression beyond and within the *P.*
293 *syringae* species complex [45,46,54,65–67]. Altogether, these pieces of evidence do not align with
294 the long-standing notion according to which "almost all virulence genes of plant pathogenic
295 bacteria [...] exhibit increased transcription at temperatures well-below the respective growth
296 optima" [38]. Such misconception has led some authors to conclude that “the increase of bacterial
297 growth in plants at elevated temperature cannot be explained by variations in intrinsic bacterial
298 growth rate or secretion of effector proteins at different temperatures. A slow HR is also unlikely
299 to be caused by a slow accumulation of bacteria or effector proteins leading to a slower detection
300 by plants” [68]. Such statements are strongly contradicted by our results, and no longer included
301 in the conclusions of other important and more recent articles that present an implicitly updated
302 perspective with which our work aligns [37,54,60].
303

304 Effector repertoire role in the lack of HR induction.

305 Although *AvrB* expression was assessed for all the strains, two of them (J35 *AvrB* and MAFF302273
306 *AvrB*) were categorized as non-inducers for at least two of the tested temperatures. While HrpZ
307 secretion data *in vitro* confirmed that J35 *AvrB*’s T3SS was unactive, the contrary was
308 demonstrated for MAFF302273 *AvrB*. Consequently, the lack of HR induction could result from the
309 T3SS inactivation in *A. thaliana*, potentially because of a quick PTI onset [27]. On the other hand,
310 it could also be a matter of speed of ETI onset, whose rapidity prevents cell death occurrence [69].
311 Otherwise, strain MAFF302273 *AvrB* may contain in its repertoire some suppressive effector(s)
312 blocking the ability of AvrB to trigger the HR [70], or some effector(s) targeting a molecular actor
313 involved in both PTI and ETI, or simply blocking the PTI – required in the first place for ETI

314 activation. Consistently we checked for effector repertoire composition for strain MAFF302273
315 (PsyTEC [71]). To the best of our knowledge, no evidence of direct or indirect antagonism between
316 AvrB and other effectors naturally present was found. However, it is not possible to exclude the
317 occurrence of 'meta-effector' interactions [20,72]. Overall, the in-depth-study of the effector
318 repertoires of all the strains used in our work could help to explain the differences observed in
319 terms of HR intensity, with one or more effectors that may inhibit HR but also enhance it
320 conversely – as observed for strain CC1498 *AvrB* versus strain CC0094 *AvrB*, for example.
321

322 **Temperature and plant immunity.**

323 Using HR induction as a proxy for T3SS efficiency, we implicitly accounted for plant defense
324 mechanisms that play a role in the response [69]. In *A. thaliana*, the role of temperature in plant
325 immunity is more complex than what reported by previous studies. In 2009, Wang and colleagues
326 concluded that a mild increase in temperature impaired both PTI and ETI, suggesting a general
327 deficiency in the plant defense system at elevated temperatures (28-30°C) [68]. Subsequently, a
328 straightforward dichotomy was established: less efficient ETI (effective from 10 to 23°C, with a
329 peak at 18°C) versus more efficient PTI (effective from 23 to 32°C, with a peak at 28°C) as the
330 temperature increases [56]. This model was later qualified by the demonstration that, since ETI
331 relies on distinct processes (*i.e.*, virulence suppression and programmed cell death/HR), only HR
332 was inhibited by elevated temperatures as the virulence suppression was maintained [73].
333 However, despite their demonstration that ion leakage from *A. thaliana* leaf disks infiltrated with
334 the avirulent DC3000 strain is completely inhibited at 28°C-30°C, our results for this *AvrB*-strain
335 and CC0094 *AvrB* and CC1498 *AvrB* contradict this finding.

336 Temperature variations may affect the kinetics of effector translocation and/or binding to R
337 proteins and hence impact the speed and efficiency of signaling cascades involved in the defense
338 response. Comparison of the ratio of conductivity values measured at 6 hpi and 24 hpi among
339 temperatures for a given HR-inducer strain revealed that the elevation of the temperature led to
340 an acceleration of electrolyte leakage as temperature increased. As this observation was
341 maintained across the strains that induced HR at different temperatures, it is tempting to associate
342 this general effect of accelerated response with the effect of the higher temperature on the plant,
343 and not on the T3SS activation or efficiency. Nevertheless, across all strains, we demonstrated that
344 some were faster than others to induce HR, also indicating some pathosystem-specific behaviors.
345

346 Temperature and effector secretion properties.

347 Interestingly, a few examples of temperature-dependency for T3SE secretion have been shown to
348 be 'protein/effector specific' – mentioning some specific secretion properties of AvrB [53].
349 Likewise, the two avirulent DC3000 strains with which HR suppression at elevated temperatures
350 was demonstrated carried either the HopZ1a or AvrRpt2 effector [73]. HopZ1a, AvrRpt2 and AvrB
351 are recognized by the NLRs ZAR1, RPS2 and RPM1, respectively, which are all members of the
352 subgroup of CC-NLRs. The unclear variability of temperature-sensitivity across different NLR
353 subgroups (CC-NLRs versus TIR-NLRs) [73,74] suggests that sensitivity may not be conserved in all
354 NLRs or CC-NLRs, given their distinct structural and functional properties. In this light, it is
355 reasonable to attribute the differences observed between our work and the one of Menna and
356 colleagues [73] to the different 'ligand-receptor' couples used. Echoing the differences in
357 'protein/effector specific' secretion efficiency, there are likely to be differences in temperature-

358 sensitivity for effector recognition by R proteins. Overall, we assume that the impact of
359 temperature on T3SS-secretion/ETI/HR-triggering efficiencies can be highly pathosystem-specific.
360 Illustrating this high specificity, DC3000 *AvrB* and M6 *AvrB* displayed a unique behavior among all
361 the tested strains. Being such strong and fast HR inducers probably reflects the fact that they are
362 highly aggressive on *A. thaliana* Col-0 (in their WT version), so the exacerbated response may also
363 be a sign of the global host compatibility between these two strains and the model plant [75,76].
364

365 Thermosensing origin and distribution among strains.

366 We attempted to identify the mechanism(s) that may be responsible for the thermosensitivity at
367 the origin of the different behaviors we observed. Two-component systems such as thermosensor
368 CorRSP responsible for the low-temperature-dependency of coronatin production in *P. syringae*
369 pv. *glycinea* could be involved in the regulation of T3SS-related gene expression in response to
370 temperature [61]. Alternatively, if evidence hints that gene expression is not directly modified by
371 temperature [55], thermoregulation might act later in the transcription/translation chain, during
372 T3SS assembly, or on translocation efficiency. In addition, the study of potential differences in
373 membrane fluidity between strains is promising. More specifically, membrane fluidity is
374 influenced by functional lipid microdomains ('FMM' or lipid rafts) that are enriched in proteins
375 involved in signal transduction and protein secretion and have the capacity to organize in space
376 and time components of transport machineries [77]. Likely, T3SS proteins co-localize on lipid rafts
377 to allow their proper assembly, and temperature would impair or favor the process, by changing
378 membrane fluidity.

379 We observed that the behavior of high temperature-preference/dependency is exclusive to strains
380 from phylogroup 2d, whereas the opposite case is specific to strains belonging to phylogroups 1a
381 and 1b. This suggests that temperature responsiveness patterns might vary among strains but
382 remain consistent within the same phylogroup. While the temperature sensitivity feature is widely
383 distributed among the strains, the preference/dependency on low or high temperatures in case
384 of thermosensitivity is conserved within a same phylogroup. This implies that the genes or targets
385 responsible for both processes may be distinct, making their identification more challenging
386 through comparative genomics. Beyond the identification of the mechanisms involved in
387 thermosensitivity, preference/dependency on low or high temperatures could be linked to the
388 evolutionary history of pathogens, which may have been shaped by temperature-related selection
389 pressures. Investigating this question would help shed light on the origin of the phenomenon.
390

391 Virulence thermoregulation in relation to disease development.

392 Since the same thermoregulation components may control various virulence factors, one
393 intriguing question is whether the effect of temperature on virulence factors is consistent (i) for a
394 given strain, and (ii) with temperature conditions in which disease occurrence is generally
395 reported. Crossing observations between temperature optimum for virulence and
396 epidemiological data regarding our selected strain revealed a high level of complexity within the
397 *P. syringae* species complex and does not allow us to draw any clearer conclusions. Concerning *P.*
398 *syringae* pv. *phaseolicola*, the low-temperature-dependency was established for phaseolotoxin
399 production and T6SS regulation, in line with the development of halo blight of bean favored at
400 temperatures below 25°C [51,78]. However, T3SS-related gene expression inhibition has been

401 reported at 18°C [50], and our results indicate that the strain 1448A is thermo-insensitive in its
402 ability to induce HR. Regarding *P. syringae* pv. *actinidiae*, our results confirmed a low-temperature
403 dependency for T3SS efficiency [55], which is entirely in line with the environmental conditions –
404 in late winter or early spring – under which *P. syringae* pv. *actinidiae* is reported to cause disease
405 or damage in the kiwifruit orchards [79,80]. On the other hand, concerning the strains CC0073
406 and CC0094 which were isolated from cantaloupe during blight epidemics in southern France in
407 the 90s, the authors have reported that the climatic conditions that favored disease outbreak and
408 development were heavy rainfall associated with a mean minimum temperature below 12-13°C
409 (under which the physiology of cantaloupe comes to a standstill) in 95% of cases, whereas our
410 results demonstrated a major T3SS efficiency at higher temperatures [81–83]. Finally, strain
411 DC3000 displays a consistent behavior, exhibiting both unaltered T3SS efficiency and coronatine
412 production in response to temperature, at least within the 18°C to 28°C range [44]. Its consistency
413 in response to various environmental parameters associated with high reproducibility of data
414 related to it have certainly contributed to making it the model strain it has become. However, this
415 strain was generated in the laboratory as a rifampicin-resistant derivative of the strain DC52,
416 which originated from Guernsey in 1960 [21,84]. Therefore, no conclusive connection could be
417 established between its ecology and its virulence behavior in response to temperature, as this
418 model strain has evolved for many years in laboratories, far from a field context.
419 Another important consideration is that our results highlighted that growth optima – at least *in*
420 *vitro* – are not correlated with T3SS efficiency. Therefore, providing a definitive answer to the
421 question of whether the temperature conditions that favor virulence (specifically T3SS) are
422 identical to those reported as favorable for disease development is challenging due to both

423 supporting and opposite examples: several traits characterizing phytopathogenic bacteria are
424 thermo-sensitive, and each pathogen is characterized by growth and virulence mechanisms that
425 are activated at precise temperatures, generating a complex scenario in which temperature can
426 alter the outcome of the interaction between plant and bacterium [60]. Consequently, we state
427 that efforts to simplify or generalize the behavior of different strains would not necessarily help
428 our understanding.
429

430 Interstrain variability.

431 One important conclusion of our work is the significant variability in behavior among strains, even
432 when closely related at the genomic level (as illustrated with the 3 'CC' strain-quasi-clones). Over
433 the years of research on these issues, examples of such inherent variability in terms of virulence
434 have been largely overlooked, with only a few cases reported in literature, both beyond and within
435 the *P. syringae* species complex [44,85–87]. This might be attributed to the commendable aim of
436 simplifying our understanding of the biological models and plant-pathogen interactions under
437 study. However, we emphasize the urgent need to study the diversity among strains, since
438 evidence of their inherent variability has been documented. Although investigating model strains
439 has facilitated the understanding and characterization of intricate molecular mechanisms in plant-
440 pathogen interactions, it is now imperative to consider the full spectrum of *P. syringae* species
441 complex diversity [3,88], both within and outside of the agronomic context.
442

443 Material & Methods

444 ## Bacterial strains and culture conditions

445 Thirteen *Pseudomonas syringae* strains were selected for this study (Table 2). These strains
446 represented four phylogroups/clades (1a, 1b, 2d, and 3a). The geographical origin and isolation
447 source of the strains varied, encompassing annual crops (*e.g.* M6, T1) [89,90], woody plants (*e.g.*
448 J35, CRA-FRU 8.43, MAFF302273) [91–93], and environmental reservoirs like rivers or snow (*e.g.*
449 LAB0041, USA007) [3,94]. Genomic relatedness within a phylogroup was also considered, aiming
450 for a balance of very divergent and closely related strains, such as the three 'CC' strains (CC0073,
451 CC0094, and CC1498) that are quasi-clones [95–97]. Model strains DC3000, B728a and 1448A
452 were also included in the set as there is a plethora of information about their biology [84,98,99].
453

454 **Table 2. Set of selected *P. syringae* strains.**

PHYLOGROUP	STRAIN	FULL NAME	ALIAS IN COLLECTIONS	ISOLATION SOURCE	COUNTRY	YEAR	REFERENCE
1a	DC3000	*P. syringae* pv. *tomato*	CFBP 7438, ICMP 18429	*Solanum lycopersicum*	United-Kingdom	1960	[84]
	M6	*P. syringae* pv. *maculicola*	CFBP 4314, NCPPB 1766, LMG 5560	*Brassica oleracea* var. Botrytis	United-Kingdom	1965	[90]
	T1	*P. syringae* pv. *tomato*	-	*Solanum lycopersicum*	Canada	1986	[89]
	LAB0041	*P. syringae*	-	Epilithic biofilm	France	2009	[3]
1b	J35	*P. syringae* pv. *actinidiae*	CFBP 4909, ICMP 9617, NCPPB 3739	*Actinidia deliciosa* cv. Hayward	Japan	1984	[93]
	CRA-FRU 8.43	*P. syringae* pv. *actinidiae*	-	*Actinidia chinensis* cv. Hort16	Italy	2008	[91]
	USA007	*P. syringae*	CFBP 8574	Creek water	United States of America	2007	[94]
2d	CC0073	*P. syringae* pv. *aptata*	CFBP 5430	*Cucumis melo*	France	1997	[95]
	CC0094	*P. syringae* pv. *aptata*	CFBP 8529	*Cucumis melo*	France	1997	[95]
	CC1498	*P. syringae*	-	Snowfall	France	2006	[96]
	B728a	*P. syringae* pv. *syringae*	CFBP 8502, ICMP 18427, NCPPB 4487, LMG 26717	*Phaseolus vulgaris*	United States of America	1987	[99]
	MAFF302273	*P. syringae* pv. *aceris*	CFBP 2339, ICMP 2802, NCPPB 958, LMG 2106	*Acer* sp.	United States of America	1939	[92]
3a	1448A	*P. syringae* pv. *phaseolicola*	CFBP 7087, NCPPB 4478	*Phaseolus vulgaris*	Ethiopia	1985	[98]

455

456 Wild-type (WT) *P. syringae* strains were grown at 28°C on King's B agar (KB) [100] – supplemented
457 with rifampicin at 50µg/mL for DC3000 and B728a strains. Kanamycin at 50µg/mL was added for

458 the culture of *AvrB* mutants. Single colonies of each strain were picked and grown overnight in
459 liquid KB medium – supplemented with rifampicin at 50µg/mL for DC3000 and B728a strains and
460 with kanamycin at 50µg/mL for *AvrB* mutants, with agitation at 190rpm at 28°C.
461

462 *AvrB*-transformation

463 Four mL of fresh WT bacterial suspension were centrifuged (5min at 4500g at 4°C) and pellets
464 were washed three times in 1mL and then resuspended in 30-50µL of sterile 10% glycerol solution
465 kept on ice. Once the pure plasmid carrying *AvrB* gene (pVB01 Km^R [62]) was added to the
466 suspensions, they underwent then an electroporation process. Once recovered, the suspensions
467 were streaked on petri dishes containing KB agar – supplemented with kanamycin at 50µg/mL for
468 all strains plus rifampicin at 50µg/mL for DC3000 and B728a strains. Plates were incubated for 48
469 up to 72 hours a 28°C. Mutant colonies were picked and *AvrB* presence was checked by PCR using
470 Promega GoTaq™ DNA polymerase (Fisher Scientific, USA) and specific primers (FOR:
471 ATGGGCTGCGTCTCGTCAAAAAGCA, REV: TTAAAAGCAATCAGAATCTAGCAAG, annealing
472 temperature = 65°C) followed by electrophoresis of the amplicons on a 1-1.5% (w/v) agarose gel.
473

474 *AvrB* expression control

475 Relative expression levels of *AvrB* among the mutant strains were evaluated by real-time PCR. Four
476 mL of fresh suspension of *AvrB*-transformed *P. syringae* strains grown overnight in selective
477 medium were centrifuged (5min at 4500g at room temperature) and total RNA was extracted from
478 bacterial pellets using TRIzol substitute (EuroGold TriFast™ Kit, EuroClone, Italy) according to
479 manufacturer instructions. Extraction yield and quality of the transcripts were checked by

480 spectrophotometric reading (NanoDrop™, Thermo Fisher Scientific, USA). Samples with
481 absorbance ratios A_{260nm}/A_{230nm} or A_{260nm}/A_{280nm} outside the range of [2 ± 0.5] were cleaned
482 following a lithium chloride RNA precipitation treatment (solution made of 7.5M LiCl, 50mM EDTA,
483 pH 8.0). 1-2µg RNA per sample underwent DNase treatment (TURBO™ DNase, Life Technologies,
484 USA) then the single-stranded complementary DNA synthesis was performed from 0.5-1µg of
485 template RNA using SuperScript™ III Reverse Transcriptase enzyme (Invitrogen, USA) according to
486 manufacturer instructions. Samples get 10-fold diluted and procedure was performed using Luna®
487 Universal qPCR Master Mix (New England Biolabs, USA) and *rpoD* housekeeping gene as reference,
488 and amplification was run on a QuantStudio™ 3 real-time PCR system (Applied Biosystems, USA)
489 (primers *AvrB* FOR: ATACTCTGCATTCGCCTCCG, REV: TCAACGACTCTGGCAAGGAC; primers *rpoD*
490 FOR: AACTTGCGTCTGGTGATCTC, REV: ATCAAGCCGATGTTGCCTTC). *AvrB* expression was
491 determined using the $2^{-\Delta\Delta Ct}$ method and normalized against *rpoD*, and fold-change for each strain
492 was established relative to the strain DC3000 *AvrB.*
493

494 Ion-leakage experiments

495 Hypersensitive response (HR) induction in *Arabidopsis thaliana* Col-0 was assessed by quantifying
496 programmed cell death through ion-leakage measurement, as previously published [101,102]
497 with slight modifications. *A. thaliana* Col-0 plants were cultivated in a mixture of peat soil and
498 perlite (4/1, v/v) in a growth chamber set at 24°C/21.5°C thermoperiod and 8 h light–16 h dark
499 photoperiod with 70% of relative humidity for 6 to 8 weeks. Three healthy plants with six 5-mm
500 leaf disks detached from a same plant with a cork borer were used for each experimental
501 condition. To recognize the plant they were detached from, leaf disks were marked with a colored

502 felt-tip and were then transferred into a 50mL tube containing 10mM $MgCl_2$ solution while
503 bacterial suspension preparation. Ten mL of fresh suspension of *AvrB*-expressing *P. syringae*
504 strains grown overnight in selective medium were centrifuged (5min at 4500g at room
505 temperature) and pellets were washed three times in 10mL of sterile 10mM $MgCl_2$ solution.
506 Optical density at 600nm was measured by spectrophotometer (Evolution™, ThermoFisher
507 Scientific, USA) and bacterial cells were finally resuspended in sterile 10mM $MgCl_2$ solution to
508 reach 10^8 CFU/mL (OD_{600nm} = 0.1; final volume = 30mL). Leaf disks were infiltrated with the
509 bacterial suspensions using a 50mL syringe or a vacuum chamber. Sterile 10mM $MgCl_2$ solution or
510 *hrp*-inducing medium (HIM; using 27mM glycerol as carbon source; pH 5.5) [103] were used as
511 negative controls. Infiltrated leaf disks were rinsed twice for 15m in 40mL of milliQ water under
512 gentle agitation (90 rpm) at room temperature to eliminate suspension/mock solution trace and
513 ions leaked due to mechanical damage. Infiltrated leaf disks were then distributed into 12-well
514 plate containing 2mL of milliQ water per well in order to have: (i) six disks per well, (ii) two disks
515 from each of the three different plants per well, (iii) three identical wells (one plate column) per
516 each experimental modality. Initial conductivity values ($\mu S.cm^{-1}$) in each well was measured prior
517 plates incubation (120 rpm; constant light of 80 $\mu mol.m^{-2}.s^{-1}$) at different temperatures (18°C, 24°C
518 and 28°C) using a compact conductometer (LAQUAtwin EC-11, HORIBA Scientific, Japan).
519 Conductivity increase was measured every 1.5-2 hours during the first 8 hours of the experiment,
520 and then twice between 18- and 24-hours post-inoculation (hpi), obtaining from 6 to 9
521 conductivity measures on average per well. Each experimental modality (*i.e.* one specific *AvrB*-
522 expressing strain infiltrated and then incubated at a certain temperature) was reproduced at least
523 three times (at least 3 `biological replicates' or `replicated experiments').

Statistical analysis

For each technical replicate, the conductivity value from the first measure was subtracted to values measured at each successive time points for normalization [55]. For each strain-temperature modality within each replicated experiment, conductivity was calculated as the average of the values of the three technical replicates for each time point, and ion-leakage curves over time were established accordingly. Area under each single conductivity progress curve was calculated (AUCPC), as well as variance and mean AUCPC per modality. Moreover, conductivity values corresponding to precisely 6 hpi and 24 hpi were calculated via linear interpolation, and the ratio 6 hpi/24 hpi was used as a dynamic parameter, indicating how fast a given strain induced HR at a given temperature. Comparison of strains with each other based on the 6 hpi/24 hpi conductivity ratio was assessed by analysis of variance (Kruskal-Wallis's test) followed by a post-hoc Dunn's test. The same procedure was conducted to compare the three different temperatures regardless of the strain. Data were represented graphically by boxplots.

Each single conductivity progress curve constituted from 6 to 9 time points and was considered as one statistical individual (*i.e.*, one iteration) to fit Linear Mixed-effects Models (LMM). This allowed us to account for the important variability among the diverse experimental replicates of a same modality and, most importantly, to consider the entire time course of electrolyte leakage, rather than focusing solely on isolated time points. The mathematical representation of LMM is: $Y = X\beta + Zu + \varepsilon$; where Y represents the dependent variable (the measured feature, *i.e.* conductivity increase), $X\beta$ stands for the fixed effects (*i.e.* the potential explanatory variables we want to assess the effect on Y), Zu stands for the random effects (all the unknown parameters that may be

546 responsible for the huge variability among the different replicated experiments and which we are
547 not directly interested to), and ε represents the residual. Using LMM in RStudio, we evaluated (i)
548 the strain effect (*i.e.* if the ion-leakage following *AvrB*-expressing strain infiltration was significantly
549 different from the ion-leakage due to mock treatment infiltration) to categorize each strain as 'HR-
550 inducer' or 'non-inducer' at each of the tested temperatures; and (ii) the temperature effect (*i.e.*
551 if the ion-leakage following *AvrB*-expressing strain infiltration was significantly different as the
552 incubation temperature changed) on the strains considered as HR-inducers at least at two of the
553 tested temperatures. In this way we estimated the values of model parameters and the associated
554 p-values.
555

556 ## *In-vitro* HrpZ secretion

557 Secretion of HrpZ *in vitro* was assessed for each strain used in ion leakage experiments. Twenty
558 mL of fresh suspension of *AvrB*-expressing *P. syringae* strains grown overnight in selective medium
559 were centrifuged (5min at 4500g at room temperature) and pellets were washed three times in
560 10mL of sterile minimal medium (HIM). Optical density at 600nm was measured with a
561 spectrophotometer (Evolution™, ThermoFisher Scientific, USA) and bacterial cells were
562 resuspended in sterile HIM to reach 7 x 10^8 CFU/mL (OD_{600nm} = 0.7; final volume = 150mL).
563 Suspensions were divided into three portions of 50mL, each was separately incubated at 18°C,
564 24°C and 28°C with agitation at 190 rpm. After 5 and 24 hours of incubation, 25mL of each
565 bacterial suspension was sampled and absorbance at 600nm was measured again (Evolution™,
566 ThermoFisher Scientific, USA). Cell-free culture supernatant was obtained by centrifugation and

567 filtration, and proteins of supernatant were then precipitated with trichloroacetic acid (TCA) as
568 previously described [104,105] with TCA final concentration at 5%.
569 Samples were mixed with loading buffer (50mM DTT) and run (10 min at 100V; 80 min at 130V)
570 through two 1.5mm 12% sodium dodecyl sulfate-polyacrylamide gel electrophoresis (SDS-PAGE),
571 either loading 25µL of each sample, or adjusting volume to load the supernatant extracted from
572 *ca.* 10^7 cells (OD_{600nm} = 0.6, final volume = 17.5µL). 180kDa-PageRuler™ (ThermoFisher Scientific,
573 USA) was used as protein ladder. One gel was used to assess total soluble protein content in each
574 sample and thus confirm the correct loading ratio: after rinsing with milli-Q water, the gel was
575 stained for 20 minutes in Coomassie R-250 staining solution (25% isoprophyl alcohol, 10% acetid
576 acid, 0.05% Coomassie R-250) and destained with 10% acetic acid until complete removal of the
577 background. The second gel was transferred onto nitrocellulose blotting membrane (GE
578 HealthCare, USA) for Western Blot analysis. The membrane was immersed for one hour at 37°C in
579 a blocking solution made of phosphate-buffered saline solution (PBS) (137mM NaCl, 2.7mM KCl,
580 10mM Na_2HPO_4, 1.8mM KH_2PO_4), supplemented with 0.05% Tween® 20 and 5% non-fat dry milk.
581 Then, the membrane was probed with the specific primary anti-HrpZ antibody [106], diluted 1:500
582 in the same blocking solution, and incubated at room temperature for 1h and a half. Following
583 primary antibody incubation, membrane was washed 3 times for 15min in PBS supplemented with
584 0.05% Tween® 20 under gentle agitation in the dark. Then, the membrane was probed for 1h at
585 room temperature in the dark using the conjugated secondary antibody to horseradish peroxidise
586 (Amersham Biosciences, USA), diluted 1:10000 in the same blocking solution. Finally, after three
587 additional washings in PBS (supplemented with 0.05% Tween® 20 for the first two), proteins were
588 visualised (Chemidoc™, ThermoFisher Scientific, USA) by enhanced chemiluminescent (ECL)

589 detection (GE HealthCare, USA). Blot pictures were analyzed using ImageLab software (BioRad,
590 USA). The intensity of each band was normalized to the intensity of the 70kDa band from the
591 ladder. When necessary, relative quantity was then normalized to the optical density measured
592 by the end of the incubation period to adjust the results to the number of cells initially present in
593 each sample.
594

595 *In-vitro* growth measurement

596 *In-vitro* bacterial growth under different temperatures was assessed for each strain. Four mL of
597 fresh suspension of *AvrB*-expressing *P. syringae* strains grown overnight in selective medium were
598 centrifuged (5min at 4500g at room temperature) and pellets were washed three times in 1mL of
599 fresh liquid KB. Optical density at 600nm was measured by spectrophotometer (Evolution™,
600 ThermoFisher Scientific, USA) and bacterial cells were then resuspended to reach 2 x 10^7 CFU/mL
601 (OD_{600nm} = 0.02; final volume = 2mL). Suspensions were aliquoted in a microtiter plate (200µL per
602 well), with 6 technical replicates per strain, and plates were incubated at 18°C, 24°C and 28°C.
603 Liquid KB (supplemented or not with the antibiotics) was used as negative control. Absorbance at
604 600nm was measured every 1.5-2 hours during the first 8 hours of the experiment, and then two
605 or three times between 18 and 24 hpi, obtaining from 6 to 9 absorbance measures per well. To
606 eliminate unspecific absorbance signals due to the color of KB medium and the antibiotics, the
607 value from the first measure was subtracted from values measured at each successive time points.
608 Absorbance was then calculated as the average of the values of the six technical replicates for
609 each time point, and bacterial growth curves over time were established accordingly. Each strain-
610 temperature modality was reproduced at least twice, except for T1.

611

612 ## Genome comparison

613 Genomes of the 13 *AvrB*-expressing strains used in ion-leakage experiments were retrieved mostly
614 from public sequence databases (Pseudomonas Genome Database and NCBI); draft genomes of
615 strains LAB0041, CC0073 and CC1498 were provided by Dr. Cindy Morris. To analyze the genomes,
616 a custom bioinformatic pipeline was created, with the help of the Nextflow framework [107]. The
617 pipeline was composed of several steps: i) the FastANI tool was used for rapid many-to-many ANI
618 calculation [108]; ii) BUSCO was used to assess both the genome quality and protein annotations
619 quality [109]; iii) the Prokka pipeline was used for the protein annotation [110]; iv) the EggNog-
620 mapper tool was used for the functional annotation [111]; and v) the Panaroo pipeline was
621 implemented for the creation of a pangenome of the 13 strains [112]. Then, the Panaroo output
622 table of gene presence/absence was exploited via an R script to produce interactive tables to
623 determine the number of total genes and specific genes per strain. These tables allowed for the
624 selection of genes present in a given strain, and queries could be performed to obtain information
625 for genes shared by strains.

626

627 # Acknowledgments

628 The authors thank Pr. Boris A. Vinatzer, Dr. Perrine Portier, Charlotte Chandeysson and Dr. Marco
629 Scortichini for kindly providing the *P. syringae* strains used in this study. We also thank Pr. Sheng-
630 Yang He for providing the antibody anti-HrpZ. Special thanks to Pr. Roberto Chignola and Dr. Davide
631 Martinetti for their help in analyzing ion-leakage data through statistical approaches. Finally, we

632 also thank the members of the laboratory of plant pathology of the University of Verona for their
633 technical support in conductivity measurements.
634

635 References

636 1. Lamichhane JR, Messéan A, Morris CE. Insights into epidemiology and control of diseases
637 of annual plants caused by the *Pseudomonas syringae* species complex. J Gen Plant Pathol.
638 2015;81: 331–350. doi:10.1007/s10327-015-0605-z
639 2. Lamichhane JR, Varvaro L, Parisi L, Audergon J-M, Morris CE. Disease and frost damage of
640 woody plants caused by *Pseudomonas syringae*. Advances in Agronomy. 2014. pp. 235–
641 295. doi:10.1016/B978-0-12-800132-5.00004-3
642 3. Berge O, Monteil CL, Bartoli C, Chandeysson C, Guilbaud C, Sands DC, et al. A user's guide
643 to a data base of the diversity of *Pseudomonas syringae* and its application to classifying
644 strains in this phylogenetic complex. PLoS One. 2014;9: e105547.
645 doi:10.1371/journal.pone.0105547
646 4. Sharma A, Gupta AK, Devi B. Current trends in management of bacterial pathogens
647 infecting plants. Antonie Van Leeuwenhoek. 2023;116: 303–326. doi:10.1007/s10482-023-
648 01809-0
649 5. Melotto M, Kunkel BN. Virulence strategies of plant pathogenic bacteria. In: Rosenberg E,
650 DeLong EF, Lory S, Stackebrandt E, Thompson F, editors. The Prokaryotes. Berlin,
651 Heidelberg: Springer Berlin Heidelberg; 2013. pp. 61–82. doi:10.1007/978-3-642-30141-
652 4_62
653 6. Roine E, Wei W, Yuan J, Nurmiaho-Lassila EL, Kalkkinen N, Romantschuk M, et al. Hrp pilus:

654 an *hrp*-dependent bacterial surface appendage produced by *Pseudomonas syringae* pv.
655 *tomato* DC3000. Proc Natl Acad Sci U S A. 1997;94: 3459–3464.
656 doi:10.1073/pnas.94.7.3459
657 7. Büttner D, He SY. Type III protein secretion in plant pathogenic bacteria. Plant Physiol.
658 2009;150: 1656–1664. doi:10.1104/PP.109.139089
659 8. Jin Q, He S-Y. Role of the Hrp pilus in type III protein secretion in *Pseudomonas syringae*.
660 Science. 2001;294: 2556–2558. doi:10.1126/science.1066397
661 9. Li CM. The Hrp pilus of *Pseudomonas syringae* elongates from its tip and acts as a conduit
662 for translocation of the effector protein HrpZ. EMBO J. 2002;21: 1909–1915.
663 doi:10.1093/emboj/21.8.1909
664 10. Cunnac S, Lindeberg M, Collmer A. *Pseudomonas syringae* type III secretion system
665 effectors: repertoires in search of functions. Curr Opin Microbiol. 2009;12: 53–60.
666 doi:10.1016/j.mib.2008.12.003
667 11. Galán JE, Collmer A. Type III secretion machines: bacterial devices for protein delivery into
668 host cells. Science. 1999;284: 1322–1328. doi:10.1126/science.284.5418.1322
669 12. Guo M, Tian F, Wamboldt Y, Alfano JR. The majority of the type III effector inventory of
670 *Pseudomonas syringae* pv. *tomato* DC3000 can suppress plant immunity. Mol Plant-
671 Microbe Interact. 2009;22: 1069–1080. doi:10.1094/MPMI-22-9-1069
672 13. Mudgett MB, Staskawicz BJ. Protein signaling via type III secretion pathways in
673 phytopathogenic bacteria. Curr Opin Microbiol. 1998;1: 109–115. doi:10.1016/S1369-
674 5274(98)80150-1
675 14. Hueck CJ. Type III protein secretion systems in bacterial pathogens of animals and plants.

676 Microbiol Mol Biol Rev. 1998;62: 379–433. doi:10.1128/mmbr.62.2.379-433.1998

677 15. Lee CA. Type III secretion systems: machines to deliver bacterial proteins into eukaryotic
678 cells? Trends Microbiol. 1997;5: 148–156. doi:10.1016/S0966-842X(97)01029-9

679 16. Guttman DS, Vinatzer BA, Sarkar SF, Ranall M V., Kettler G, Greenberg JT. A functional
680 screen for the type III (Hrp) secretome of the plant pathogen *Pseudomonas syringae*.
681 Science. 2002;295: 1722–1726. doi:10.1126/science.295.5560.1722

682 17. Chang JH, Urbach JM, Law TF, Arnold LW, Hu A, Gombar S, et al. A high-throughput, near-
683 saturating screen for type III effector genes from *Pseudomonas syringae*. Proc Natl Acad
684 Sci U S A. 2005;102: 2549–2554. doi:10.1073/pnas.0409660102

685 18. Xin X-F, Nomura K, Aung K, Velásquez AC, Yao J, Boutrot F, et al. Bacteria establish an
686 aqueous living space in plants crucial for virulence. Nature. 2016;539: 524–529.
687 doi:10.1038/nature20166

688 19. Lindeberg M, Cunnac S, Collmer A. *Pseudomonas syringae* type III effector repertoires: last
689 words in endless arguments. Trends Microbiol. 2012;20: 199–208.
690 doi:10.1016/j.tim.2012.01.003

691 20. Martel A, Laflamme B, Breit-McNally C, Wang P, Lonjon F, Desveaux D, et al. Metaeffector
692 interactions modulate the type III effector-triggered immunity load of *Pseudomonas*
693 *syringae*. PLoS Pathog. 2022;18: e1010541. doi:10.1371/JOURNAL.PPAT.1010541

694 21. Xin X-F, Kvitko B, He SY. *Pseudomonas syringae*: what it takes to be a pathogen. Nat Rev
695 Microbiol. 2018;16: 316–328. doi:10.1038/nrmicro.2018.17

696 22. Morris CE, Lamichhane JR, Nikolić I, Stanković S, Moury B. The overlapping continuum of
697 host range among strains in the *Pseudomonas syringae* complex. Phytopathol Res. 2019;1:

698 4. doi:10.1186/s42483-018-0010-6

699 23. Baltrus DA, McCann HC, Guttman DS. Evolution, genomics and epidemiology of
700 *Pseudomonas syringae*. Mol Plant Pathol. 2017;18: 152–168. doi:10.1111/MPP.12506

701 24. Ruiz-Bedoya T, Wang PW, Desveaux D, Guttman DS. Cooperative virulence via the collective
702 action of secreted pathogen effectors. Nat Microbiol. 2023;8: 640–650.
703 doi:10.1038/s41564-023-01328-8

704 25. Cui H, Xiang T, Zhou JM. Plant immunity: a lesson from pathogenic bacterial effector
705 proteins. Cell Microbiol. 2009;11: 1453–1461. doi:10.1111/J.1462-5822.2009.01359.X

706 26. Boller T, Felix G. A renaissance of elicitors: perception of Microbe-Associated Molecular
707 Patterns and danger signals by Pattern-Recognition Receptors. Annu Rev Plant Biol.
708 2009;60: 379–406. doi:10.1146/annurev.arplant.57.032905.105346

709 27. Crabill E, Joe A, Block A, van Rooyen JM, Alfano JR. Plant immunity directly or indirectly
710 restricts the injection of type III effectors by the *Pseudomonas syringae* type III secretion
711 system. Plant Physiol. 2010;154: 233–244. doi:10.1104/pp.110.159723

712 28. Anderson JC, Wan Y, Kim Y-M, Pasa-Tolic L, Metz TO, Peck SC. Decreased abundance of
713 type III secretion system-inducing signals in *Arabidopsis mkp1* enhances resistance against
714 *Pseudomonas syringae*. Proc Natl Acad Sci. 2014;111: 6846–6851.
715 doi:10.1073/pnas.1403248111

716 29. Thomma BPHJ, Nürnberger T, Joosten MHAJ. Of PAMPs and effectors: the blurred PTI-ETI
717 dichotomy. Plant Cell. 2011;23: 4–15. doi:10.1105/tpc.110.082602

718 30. Monteiro F, Nishimura MT. Structural, functional, and genomic diversity of plant NLR
719 proteins: an evolved resource for rational engineering of plant immunity. Annu Rev

720 Phytopathol. 2018;56: 243–267. doi:10.1146/annurev-phyto-080417-045817

721 31. Jones JDG, Dangl JL. The plant immune system. Nature. 2006;444: 323–329.
722 doi:10.1038/nature05286

723 32. Ngou BPM, Ahn H-K, Ding P, Jones JDG. Mutual potentiation of plant immunity by cell-
724 surface and intracellular receptors. Nature. 2021;592: 110–115. doi:10.1038/s41586-021-
725 03315-7

726 33. Yuan M, Jiang Z, Bi G, Nomura K, Liu M, Wang Y, et al. Pattern-recognition receptors are
727 required for NLR-mediated plant immunity. Nature. 2021;592: 105–109.
728 doi:10.1038/s41586-021-03316-6

729 34. Balint-Kurti P. The plant hypersensitive response: concepts, control and consequences. Mol
730 Plant Pathol. 2019;20: 1163–1178. doi:10.1111/mpp.12821

731 35. Coll NS, Epple P, Dangl JL. Programmed cell death in the plant immune system. Cell Death
732 Differ. 2011;18: 1247–1256. doi:10.1038/cdd.2011.37

733 36. Stevens RB. JG Horsfall and AE Dimond, eds. Plant Pathology, an Advanced Treatise, Vol 3.
734 Academic Press, NY; 1960. pp. 357–429.

735 37. Velásquez AC, Castroverde CDM, He SY. Plant–pathogen warfare under changing climate
736 conditions. Current Biology. Cell Press; 2018. pp. R619–R634.
737 doi:10.1016/j.cub.2018.03.054

738 38. Smirnova A, Li H, Weingart H, Aufhammer S, Burse A, Finis K, et al. Thermoregulated
739 expression of virulence factors in plant-associated bacteria. Arch Microbiol. 2001;176:
740 393–399. doi:10.1007/s002030100344

741 39. Hockett KL, Burch AY, Lindow SE. Thermo-regulation of genes mediating motility and plant

742 interactions in *Pseudomonas syringae*. PLoS One. 2013;8: e59850.
743 doi:10.1371/journal.pone.0059850
744 40. Aguilera S, Alvarez-Morales A, Murillo J, Hernández-Flores JL, Bravo J, De la Torre-Zavala S.
745 Temperature-mediated biosynthesis of the phytotoxin phaseolotoxin by *Pseudomonas*
746 *syringae* pv. *phaseolicola* depends on the autoregulated expression of the *phtABC* genes.
747 PLoS One. 2017;12: e0178441. doi:10.1371/journal.pone.0178441
748 41. Palmer DA, Bender CL. Effects of environmental and nutritional factors on production of
749 the polyketide phytotoxin coronatine by *Pseudomonas syringae* pv. *glycinea*. Appl Environ
750 Microbiol. 1993;59: 1619–1626. doi:10.1128/aem.59.5.1619-1626.1993
751 42. Ullrich MS, Schergaut M, Boch J, Ullrich B. Temperature-responsive genetic loci in the plant
752 pathogen *Pseudomonas syringae* pv. *glycinea*. Microbiology. 2000;146: 2457–2468.
753 doi:10.1099/00221287-146-10-2457
754 43. Braun Y, Smirnova A V., Weingart H, Schenk A, Ullrich MS. Coronatine gene expression *in*
755 *vitro* and *in planta*, and protein accumulation during temperature downshift in
756 *Pseudomonas syringae*. Sensors. 2009;9: 4272–4285. doi:10.3390/s90604272
757 44. Weingart H, Stubner S, Schenk A, Ullrich MS. Impact of temperature on *in planta* expression
758 of genes involved in synthesis of the *Pseudomonas syringae* phytotoxin coronatine. Mol
759 Plant-Microbe Interact. 2004;17: 1095–1102. doi:10.1094/MPMI.2004.17.10.1095
760 45. Krishna PS, Woodcock SD, Pfeilmeier S, Bornemann S, Zipfel C, Malone JG. *Pseudomonas*
761 *syringae* addresses distinct environmental challenges during plant infection through the
762 coordinated deployment of polysaccharides. J Exp Bot. 2022;73: 2206–2221.
763 doi:10.1093/jxb/erab550

764 46. Peñaloza-Vázquez A, Kidambi SP, Chakrabarty AM, Bender CL. Characterization of the
765 alginate biosynthetic gene cluster in *Pseudomonas syringae* pv. *syringae*. J Bacteriol.
766 1997;179: 4464–4472. doi:10.1128/jb.179.14.4464-4472.1997
767 47. Li H, Schenk A, Srivastava A, Zhurina D, Ullrich MS. Thermo-responsive expression and
768 differential secretion of the extracellular enzyme levansucrase in the plant pathogenic
769 bacterium *Pseudomonas syringae* pv. *glycinea*. FEMS Microbiol Lett. 2006;265: 178–185.
770 doi:10.1111/J.1574-6968.2006.00486.X
771 48. Scalschi L, Fernández-Crespo E, Pitarch-Marin M, Llorens E, González-Hernández AI,
772 Camañes G, et al. Response of tomato-*Pseudomonas* pathosystem to mild heat stress.
773 Horticulturae. 2022;8: 174. doi:10.3390/horticulturae8020174
774 49. Bender CL, Alarcón-Chaidez F, Gross DC. *Pseudomonas syringae* phytotoxins: mode of
775 action, regulation, and biosynthesis by peptide and polyketide synthetases. Microbiol Mol
776 Biol Rev. 1999;63: 266–292. doi:10.1128/MMBR.63.2.266-292.1999
777 50. Arvizu-Gómez JL, Hernández-Morales A, Aguilar JRP, Álvarez-Morales A. Transcriptional
778 profile of *P. syringae* pv. *phaseolicola* NPS3121 at low temperature: physiology of
779 phytopathogenic bacteria. BMC Microbiol. 2013;13: 81. doi:10.1186/1471-2180-13-81
780 51. Nüske J, Fritsche W. Phaseolotoxin production by *Pseudomonas syringae* pv. *phaseolicola*:
781 the influence of temperature. J Basic Microbiol. 1989;29: 441–447.
782 doi:10.1002/JOBM.3620290713
783 52. Aguilera S, López-López K, Nieto Y, Garcidueñas-Piña R, Hernández-Guzmán G, Hernández-
784 Flores JL, et al. Functional characterization of the gene cluster from *Pseudomonas syringae*
785 pv. *phaseolicola* NPS3121 involved in synthesis of phaseolotoxin. J Bacteriol. 2007;189:

786 2834. doi:10.1128/JB.01845-06

787 53. Van Dijk K, Fouts DE, Rehm AH, Hill AR, Collmer A, Alfano JR. The Avr (effector) proteins
788 HrmA (HopPsyA) and AvrPto are secreted in culture from *Pseudomonas syringae* pathovars
789 via the Hrp (type III) protein secretion system in a temperature- and pH-sensitive manner.
790 J Bacteriol. 1999;181: 4790–4797. doi:10.1128/jb.181.16.4790-4797.1999

791 54. Huot B, Castroverde CDM, Velásquez AC, Hubbard E, Pulman JA, Yao J, et al. Dual impact
792 of elevated temperature on plant defence and bacterial virulence in *Arabidopsis*. Nat
793 Commun. 2017;8: 1808. doi:10.1038/s41467-017-01674-2

794 55. Puttilli MR, Danzi D, Correia C, Brandi J, Cecconi D, Manfredi M, et al. Plant signals
795 anticipate the induction of the type III secretion system in *Pseudomonas syringae* pv.
796 *actinidiae*, facilitating efficient temperature-dependent effector translocation. Microbiol
797 Spectr. 2022;10. doi:10.1128/spectrum.02073-22

798 56. Cheng C, Gao X, Feng B, Sheen J, Shan L, He P. Plant immune response to pathogens differs
799 with changing temperatures. Nat Commun. 2013;4: 2530. doi:10.1038/ncomms3530

800 57. Klinkert B, Narberhaus F. Microbial thermosensors. Cellular and Molecular Life Sciences.
801 Springer; 2009. pp. 2661–2676. doi:10.1007/s00018-009-0041-3

802 58. Jin S, Song YN, Deng WY, Gordon MP, Nester EW. The regulatory VirA protein of
803 *Agrobacterium tumefaciens* does not function at elevated temperatures. J Bacteriol.
804 1993;175: 6830–6835. doi:10.1128/JB.175.21.6830-6835.1993

805 59. Arvizu-Gómez JL, Hernández-Morales A, Jofre-Garfias AE, Álvarez-Morales A. Temperature,
806 the GacS/GacA system, and host metabolites regulate the type VI secretion system of
807 *Pseudomonas syringae* pv. *phaseolicola*. J Gen Plant Pathol. 2013;79: 194–197.

808 doi:10.1007/s10327-013-0443-9

809 60. Tribelli PM, López NI. Insights into the temperature responses of *Pseudomonas* species in
810 beneficial and pathogenic host interactions. Applied Microbiology and Biotechnology.
811 2022. pp. 7699–7709. doi:10.1007/s00253-022-12243-z

812 61. Ullrich M, Penaloza-Vazquez A, Bailey AM, Bender CL. A modified two-component
813 regulatory system is involved in temperature- dependent biosynthesis of the *Pseudomonas*
814 *syringae* phytotoxin coronatine. J Bacteriol. 1995;177: 6160–6169.
815 doi:10.1128/jb.177.21.6160-6169.1995

816 62. Innes RW, Bisgrove SR, Smith NM, Bent AF, Staskawicz BJ, Liu Y. Identification of a disease
817 resistance locus in *Arabidopsis* that is functionally homologous to the *RPG1* locus of
818 soybean. Plant J. 1993;4: 813–820. doi:10.1046/j.1365-313X.1993.04050813.x

819 63. Mudgett MB. New insights to the function of phytopathogenic bacterial type III effectors
820 in plants. Annual Review of Plant Biology. Annual Reviews; 2005. pp. 509–531.
821 doi:10.1146/annurev.arplant.56.032604.144218

822 64. Mackey D, Holt BF, Wiig A, Dangl JL. RIN4 interacts with *Pseudomonas syringae* type III
823 effector molecules and is required for RPM1-mediated resistance in *Arabidopsis*. Cell.
824 2002;108: 743–754. doi:10.1016/S0092-8674(02)00661-X

825 65. Wei M, Yokoyama T, Minamisawa K, Mitsui H, Itakura M, Kaneko T, et al. Soybean seed
826 extracts preferentially express genomic loci of *Bradyrhizobium japonicum* in the initial
827 interaction with soybean, *Glycine max* (L.) Merr. DNA Res. 2008;15: 201–214.
828 doi:10.1093/dnares/dsn012

829 66. Wei M, KeisukeTakeshima, Yokoyama T, Minamisawa K, Mitsui H, Itakura M, et al.

830 Temperature-dependent expression of type III secretion system genes and its regulation in
831 *Bradyrhizobium japonicum*. Mol Plant-Microbe Interact. 2010;23: 628–637.
832 doi:10.1094/MPMI-23-5-0628
833 67. Czajkowski R, Kaczyńska N, Jafra S, Narajczyk M, Lojkowska E. Temperature-responsive
834 genetic loci in pectinolytic plant pathogenic *Dickeya solani*. Plant Pathol. 2017;66: 584–594.
835 doi:10.1111/PPA.12618
836 68. Wang Y, Bao Z, Zhu Y, Hua J. Analysis of temperature modulation of plant defense against
837 biotrophic microbes. Mol Plant-Microbe Interact. 2009;22: 498–506. doi:10.1094/MPMI-
838 22-5-0498
839 69. Künstler A, Bacsó R, Gullner G, Hafez YM, Király L. Staying alive – is cell death dispensable
840 for plant disease resistance during the hypersensitive response? Physiol Mol Plant Pathol.
841 2016;93: 75–84. doi:10.1016/j.pmpp.2016.01.003
842 70. Jamir Y, Guo M, Oh H, Petnicki-Ocwieja T, Chen S, Tang X, et al. Identification of
843 *Pseudomonas syringae* type III effectors that can suppress programmed cell death in plants
844 and yeast. Plant J. 2004;37: 554–565. doi:10.1046/j.1365-313X.2003.01982.x
845 71. Laflamme B, Dillon MM, Martel A, Almeida RND, Desveaux D, Guttman DS. The pan-
846 genome effector-triggered immunity landscape of a host-pathogen interaction. Science.
847 2020;367: 763–768. doi:10.1126/science.aax4079
848 72. Kubori T, Shinzawa N, Kanuka H, Nagai H. *Legionella* metaeffector exploits host proteasome
849 to temporally regulate cognate effector. PLoS Pathog. 2010;6: e1001216.
850 doi:10.1371/journal.ppat.1001216
851 73. Menna A, Nguyen D, Guttman DS, Desveaux D. Elevated temperature differentially

852 influences effector-triggered immunity outputs in *Arabidopsis*. Front Plant Sci. 2015;6: 1–
853 7. doi:10.3389/fpls.2015.00995
854 74. Hua J. Temperature and plant immunity. Temperature and Plant Development. Wiley;
855 2014. pp. 163–180. doi:10.1002/9781118308240.ch7
856 75. Preston GM. *Pseudomonas syringae* pv. *tomato* : the right pathogen, of the right plant, at
857 the right time. Mol Plant Pathol. 2000;1: 263–275. doi:10.1046/j.1364-3703.2000.00036.x
858 76. Xin XF, He SY. *Pseudomonas syringae* pv. *tomato* DC3000: a model pathogen for probing
859 disease susceptibility and hormone signaling in plants. Annu Rev Phytopathol. 2013;51:
860 473–498. doi:10.1146/annurev-phyto-082712-102321
861 77. Bramkamp M, Lopez D. Exploring the existence of lipid rafts in bacteria. Microbiol Mol Biol
862 Rev. 2015;79: 81–100. doi:10.1128/mmbr.00036-14
863 78. Goss RW. The relation of temperature to common and halo blight of beans.
864 Phytopathology. 1940;30: 258–264.
865 79. Kim GH, Jung JS, Koh YJ. Occurrence and epidemics of bacterial canker of kiwifruit in Korea.
866 Plant Pathol J. 2017;33: 351–361. doi:10.5423/PPJ.RW.01.2017.0021
867 80. Donati I, Cellini A, Sangiorgio D, Vanneste JL, Scortichini M, Balestra GM, et al.
868 *Pseudomonas syringae* pv. *actinidiae*: ecology, infection dynamics and disease
869 epidemiology. Microb Ecol. 2020;80: 81–102. doi:10.1007/s00248-019-01459-8
870 81. Morris CE, Pitrat M. La bactériose du melon : connaissances acquises et travaux en cours.
871 PHM Rev Hortic. 1998; 44–47.
872 82. Riffaud C. La bactériose du melon : écologie et stratégies de lutte contre *Pseudomonas*
873 *syringae* pv.*aptata*. Université Claude Bernard Lyon I. 2002.

874 83. Mention P, Lavigne D, Leix-Henry F, Bouchu S, Morris CE, Prior P, et al. Bactériose du melon:
875 acquis et perspectives. PHM Rev Hortic. 2004; 22–26.
876 84. Cuppels DA. Generation and characterization of Tn5 insertion mutations in *Pseudomonas*
877 *syringae* pv. *tomato*. Appl Environ Microbiol. 1986;51: 323–327.
878 doi:10.1128/aem.51.2.323-327.1986
879 85. Baron C, Domke N, Beinhofer M, Hapfelmeier S. Elevated temperature differentially affects
880 virulence, VirB protein accumulation, and T-pilus formation in different *Agrobacterium*
881 *tumefaciens* and *Agrobacterium vitis* strains. J Bacteriol. 2001;183: 6852–6861.
882 doi:10.1128/JB.183.23.6852-6861.2001
883 86. Hasegawa H, Chatterjee A, Cui Y, Chatterjee AK. Elevated temperature enhances virulence
884 of *Erwinia carotovora* subsp. *carotovora* strain EC153 to plants and stimulates production
885 of the quorum sensing signal, N -acyl homoserine lactone, and extracellular proteins. Appl
886 Environ Microbiol. 2005;71: 4655–4663. doi:10.1128/AEM.71.8.4655-4663.2005
887 87. Rohde BH, Pohlack B, Ullrich MS. Occurrence of thermoregulation of genes involved in
888 coronatine biosynthesis among various *Pseudomonas syringae* strains. J Basic Microbiol.
889 1998;38: 41–50. doi:10.1002/(SICI)1521-4028(199803)38:1<41::AID-JOBM41>3.0.CO;2-6
890 88. Gomila M, Busquets A, Mulet M, García-Valdés E, Lalucat J. Clarification of taxonomic
891 status within the *Pseudomonas syringae* species group based on a phylogenomic analysis.
892 Front Microbiol. 2017;8: 320397. doi:10.3389/fmicb.2017.02422
893 89. Whalen MC, Innes RW, Bent AF, Staskawicz BJ. Identification of *Pseudomonas syringae*
894 pathogens of *Arabidopsis* and a bacterial locus determining avirulence on both *Arabidopsis*
895 and soybean. Plant Cell. 1991;3: 49. doi:10.1105/TPC.3.1.49

896 90. Debener T, Lehnackers H, Arnold M, Dangl JL. Identification and molecular mapping of a
897 single *Arabidopsis thaliana* locus determining resistance to a phytopathogenic
898 *Pseudomonas syringae* isolate. Plant J. 1991;1: 289–302. doi:10.1046/J.1365-
899 313X.1991.T01-7-00999.X
900 91. Ferrante P, Scortichini M. Molecular and phenotypic features of *Pseudomonas syringae* pv.
901 *actinidiae* isolated during recent epidemics of bacterial canker on yellow kiwifruit (*Actinidia*
902 *chinensis*) in central Italy. Plant Pathol. 2010;59: 954–962. doi:10.1111/j.1365-
903 3059.2010.02304.x
904 92. Sawada H, Suzuki F, Matsuda I, Saitou N. Phylogenetic analysis of *Pseudomonas syringae*
905 pathovars suggests the horizontal gene transfer of *argK* and the evolutionary stability of
906 *hrp* gene cluster. J Mol Evol. 1999;49: 627–644. doi:10.1007/PL00006584
907 93. Takikawa Y, Serizawa S, Ichikawa T, Tsuyumu S, Goto M. *Pseudomonas syringae* pv.
908 *actinidiae* pv. nov.: the causal bacterium of canker of kiwifruit in Japan. Japanese J
909 Phytopathol. 1989;55: 437–444. doi:10.3186/jjphytopath.55.437
910 94. Morris CE, Sands DC, Vanneste JL, Montarry J, Oakley B, Guilbaud C, et al. Inferring the
911 evolutionary history of the plant pathogen *Pseudomonas syringae* from its biogeography
912 in headwaters of rivers in North America, Europe, and New Zealand. MBio. 2010;1.
913 doi:10.1128/mBio.00107-10
914 95. Morris CE, Glaux C, Latour X, Gardan L, Samson R, Pitrat M. The relationship of host range,
915 physiology, and genotype to virulence on cantaloupe in *Pseudomonas syringae* from
916 cantaloupe blight epidemics in France. Phytopathology. 2000;90: 636–646.
917 doi:10.1094/PHYTO.2000.90.6.636

918 96. Morris CE, Sands DC, Vinatzer BA, Glaux C, Guilbaud C, Buffière A, et al. The life history of
919 the plant pathogen *Pseudomonas syringae* is linked to the water cycle. ISME J. 2008;2: 321–
920 334. doi:10.1038/ismej.2007.113
921 97. Monteil CL, Yahara K, Studholme DJ, Mageiros L, Méric G, Swingle B, et al. Population-
922 genomic insights into emergence, crop adaptation and dissemination of *Pseudomonas*
923 *syringae* pathogens. Microb Genomics. 2016;2: e000089. doi:10.1099/mgen.0.000089
924 98. Taylor JD, Teverson DM, Allen DJ, Pastor-Corrales MA. Identification and origin of races of
925 *Pseudomonas syringae* pv. *phaseolicola* from Africa and other bean growing areas. Plant
926 Pathol. 1996;45: 469–478. doi:10.1046/J.1365-3059.1996.D01-147.X
927 99. Loper JE, Lindow SE. Lack of evidence for *in situ* fluorescent pigment production by
928 *Pseudomonas syringae* pv. *syringae* on bean leaf surfaces. Phytopathology. 1987;77: 1449.
929 doi:10.1094/phyto-77-1449
930 100. King EO, Ward MK, Raney DE. Two simple media for the demonstration of pyocyanin and
931 fluorescin. J Lab Clin Med. 1954;44: 301–307.
932 101. Imanifard Z, Vandelle E, Bellin D. Measurement of hypersensitive cell death triggered by
933 avirulent bacterial pathogens in *Arabidopsis*. Methods Mol Biol. 2018;1743: 39–50.
934 doi:10.1007/978-1-4939-7668-3_4
935 102. Johansson ON, Nilsson AK, Gustavsson MB, Backhaus T, Andersson MX, Ellerström M. A
936 quick and robust method for quantification of the hypersensitive response in plants. PeerJ.
937 2015;3: e1469. doi:10.7717/peerj.1469
938 103. Huynh T V., Dahlbeck D, Staskawicz BJ. Bacterial blight of soybean: regulation of a pathogen
939 gene determining host cultivar specificity. Science. 1989;245: 1374–1377.

940 doi:10.1126/science.2781284

941 104. Flaugnatti N, Journet L. Identification of effectors: precipitation of supernatant material.
942 Bacterial Protein Secretion Systems. 2017. pp. 459–464. doi:10.1007/978-1-4939-7033-
943 9_31

944 105. Kobayashi T, Kishigami S, Sone M, Inokuchi H, Mogi T, Ito K. Respiratory chain is required
945 to maintain oxidized states of the DsbA-DsbB disulfide bond formation system in
946 aerobically growing *Escherichia coli* cells. Proc Natl Acad Sci U S A. 1997;94: 11857–11862.
947 doi:10.1073/pnas.94.22.11857

948 106. Alfano JR, Bauer DW, Milos TM, Collmer A. Analysis of the role of the *Pseudomonas*
949 *syringae* pv. *syringae* HrpZ harpin in elicitation of the hypersensitive response in tobacco
950 using functionally non-polar *hrpZ* deletion mutations, truncated HrpZ fragments, and *hrmA*
951 mutatio. Mol Microbiol. 1996;19: 715–728. doi:10.1046/j.1365-2958.1996.415946.x

952 107. Di Tommaso P, Chatzou M, Floden EW, Barja PP, Palumbo E, Notredame C. Nextflow
953 enables reproducible computational workflows. Nature Biotechnology. Nature Publishing
954 Group; 2017. pp. 316–319. doi:10.1038/nbt.3820

955 108. Jain C, Rodriguez-R LM, Phillippy AM, Konstantinidis KT, Aluru S. High throughput ANI
956 analysis of 90K prokaryotic genomes reveals clear species boundaries. Nat Commun.
957 2018;9: 5114. doi:10.1038/s41467-018-07641-9

958 109. Manni M, Berkeley MR, Seppey M, Simão FA, Zdobnov EM. BUSCO update: novel and
959 streamlined workflows along with broader and deeper phylogenetic coverage for scoring
960 of eukaryotic, prokaryotic, and viral genomes. Mol Biol Evol. 2021;38: 4647–4654.
961 doi:10.1093/molbev/msab199

110. Seemann T. Prokka: rapid prokaryotic genome annotation. Bioinformatics. 2014;30: 2068–2069. doi:10.1093/bioinformatics/btu153

111. Cantalapiedra CP, Hernandez-Plaza A, Letunic I, Bork P, Huerta-Cepas J. eggNOG-mapper v2: functional annotation, orthology assignments, and domain prediction at the metagenomic scale. Mol Biol Evol. 2021;38: 5825–5829. doi:10.1093/molbev/msab293

112. Tonkin-Hill G, MacAlasdair N, Ruis C, Weimann A, Horesh G, Lees JA, et al. Producing polished prokaryotic pangenomes with the Panaroo pipeline. Genome Biol. 2020;21: 1–21. doi:10.1186/s13059-020-02090-4

Supporting information captions

S1 Fig. Variance of the mean area under conductivity progress curve (AUCPC) values obtained for each 39 modalities *AvrB*-expressing strain x temperature. Number of replicated experiments for each strain varied from 3 up to 27. Linear regression trend curve was fitted to the data, with $y=323.89x - 150932$ and $R^2=0.8588$, showing a positive correlation between mean AUCPC and their variance (Spearman's coefficient = 0.91; $p < 0.05$).

S2 Fig. *AvrB* expression among the mutant strains. RNA was extracted from bacterial suspensions grown overnight at 28°C in liquid KB medium supplemented with kanamycin (50µg/mL) and rifampicin (50µg/mL, for DC3000 *AvrB* and B728a *AvrB* only). Real-time PCR was performed using *rpoD* as the housekeeping gene. Expression levels were established using the $2^{-\Delta\Delta Ct}$ method using

983 DC3000 *AvrB* as a reference (fold change = 1). Error bars represent standard error. Data represent
984 the mean of three independent biological replicates, each repeated at least twice.
985
986 **S3 Fig. *In-vitro* growth curves for DC3000 *AvrB* (A), USA007 *AvrB* (B) and CC0094 *AvrB* (C)**.
987 Bacterial growth was measured for 24 hours at 18°C (blue), 24°C (pink) and 28°C (red). Overnight
988 grown bacteria were resuspended in liquid KB medium supplemented with kanamycin (50µg/mL)
989 and rifampicin (50µg/mL, for DC3000 *AvrB* only) at an initial load of 10^7 CFU/mL (optical density
990 measured at 600nm = 0.01). Data represent one single representative biological replicate with all
991 strains and temperature conditions evaluated simultaneously with six technical replicates each.
992 Error bars represent standard error.
993
994 **S4 Fig. HrpZ secretion profiles across a range of temperature.** *AvrB*-expressing strains were
995 incubated in *hrp*-inducing medium (HIM) at 18°C, 24°C or 28°C for 5 hours. Cell-free culture
996 supernatant was obtained by centrifugation and filtration. Proteins of bacterial culture
997 supernatant were then precipitated with trichloroacetic acid (TCA) and analyzed by Western blot
998 using an anti-HrpZ antibody. The expected molecular weight is *ca*. 40kDa. A mix of samples proven
999 to contain HrpZ in previous replicates was used as the positive control (C+) at two different
1000 concentrations (1X and 2X). Samples were run in different gels that were transferred onto
1001 membranes whose pictures were cropped and merged into a single figure.
1002
1003 **S5 Fig. Ratios of conductivity increase measured at 6 hpi and 24 hpi for all *AvrB*-expressing**
1004 **strains inducing HR at least at one temperature condition, at each of the temperatures.** Boxes

1005 were calculated from 70 to 97 replicated experiments per temperature (single dots). Boxes
1006 associated with different letters represent significantly different means ($p < 0.05$, according to a
1007 Kruskal-Wallis's test followed by post-hoc Dunn's test).
1008
1009 **S1 Table. List of the 10 genes with available annotation present in strains CC0094 and CC1498**
1010 **and missing in strain CC0073.** Four out of these ten genes are also present in other strains.

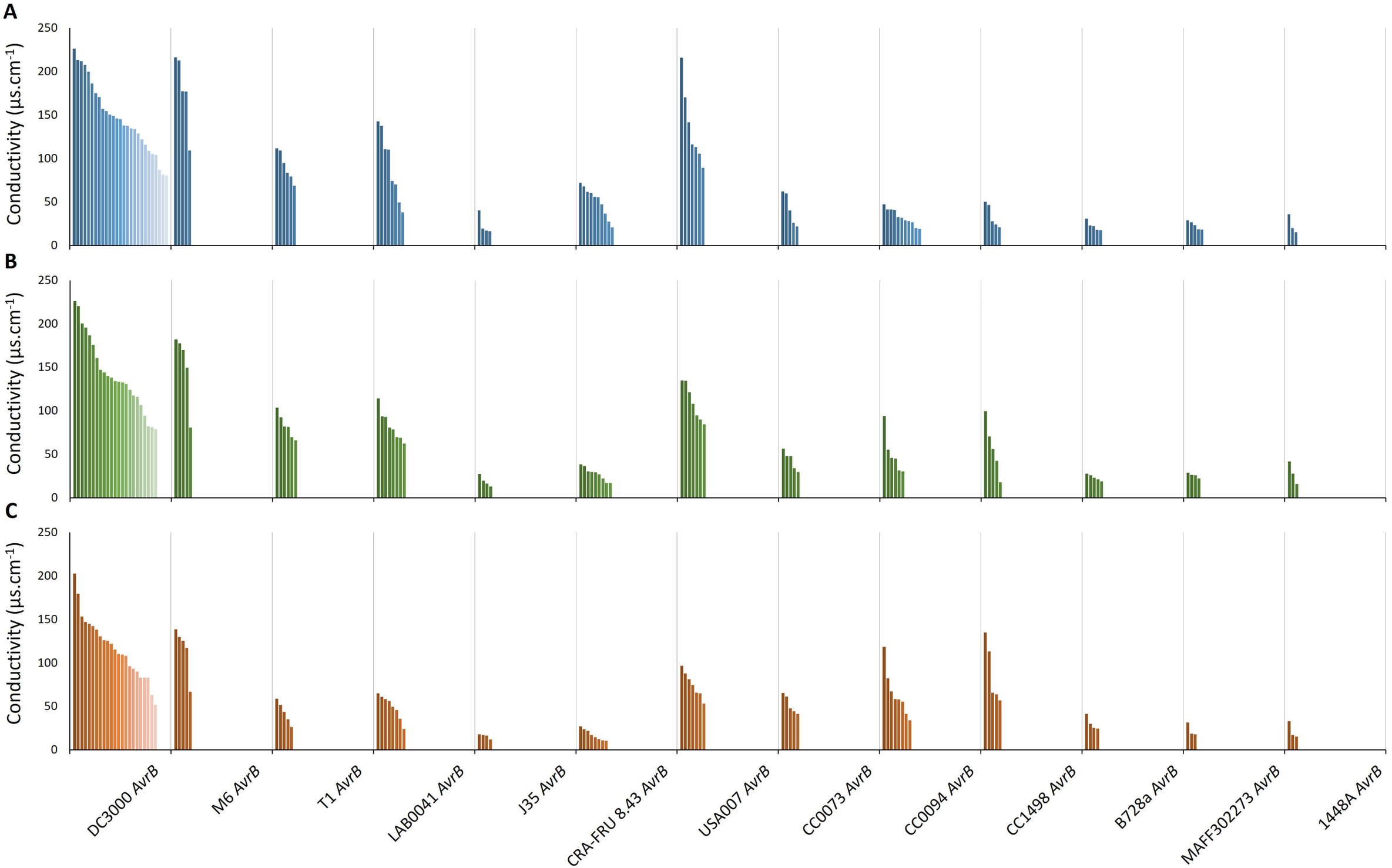
A
B
C
Conductivity (µs.cm-1)
250
200
150
100
50
0
DC3000 AvrB
M6 AvrB
T1 AvrB
LAB0041 AvrB
J35 AvrB
CRA-FRU 8.43 AvrB
USA007 AvrB
CC0073 AvrB
CC0094 AvrB
CC1498 AvrB
B728a AvrB
MAFF302273 AvrB
1448A AvrB

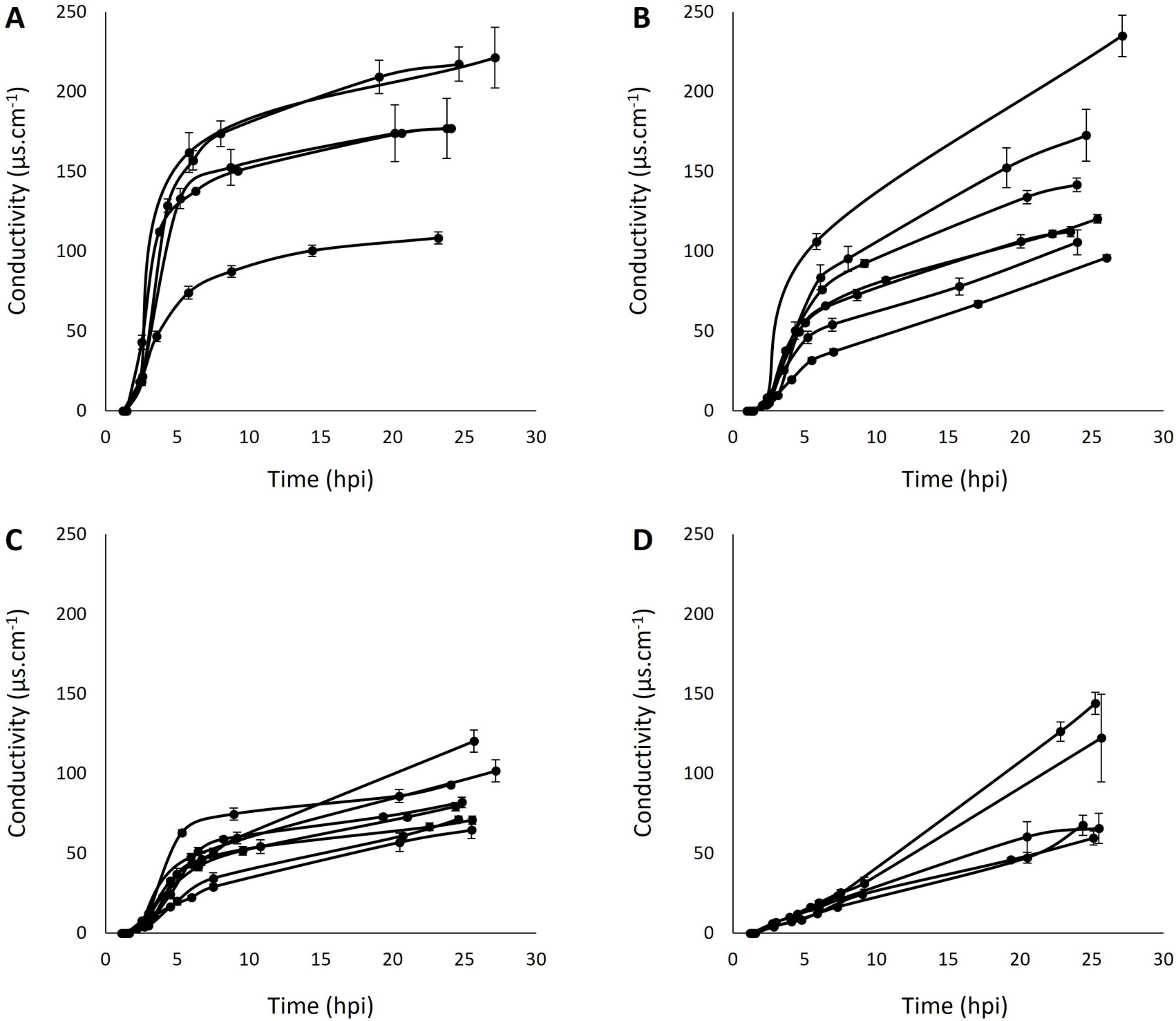
A
B
C
D
Conductivity (µs.cm-1)
Time (hpi)
0
50
100
150
200
250
0
5
10
15
20
25
30

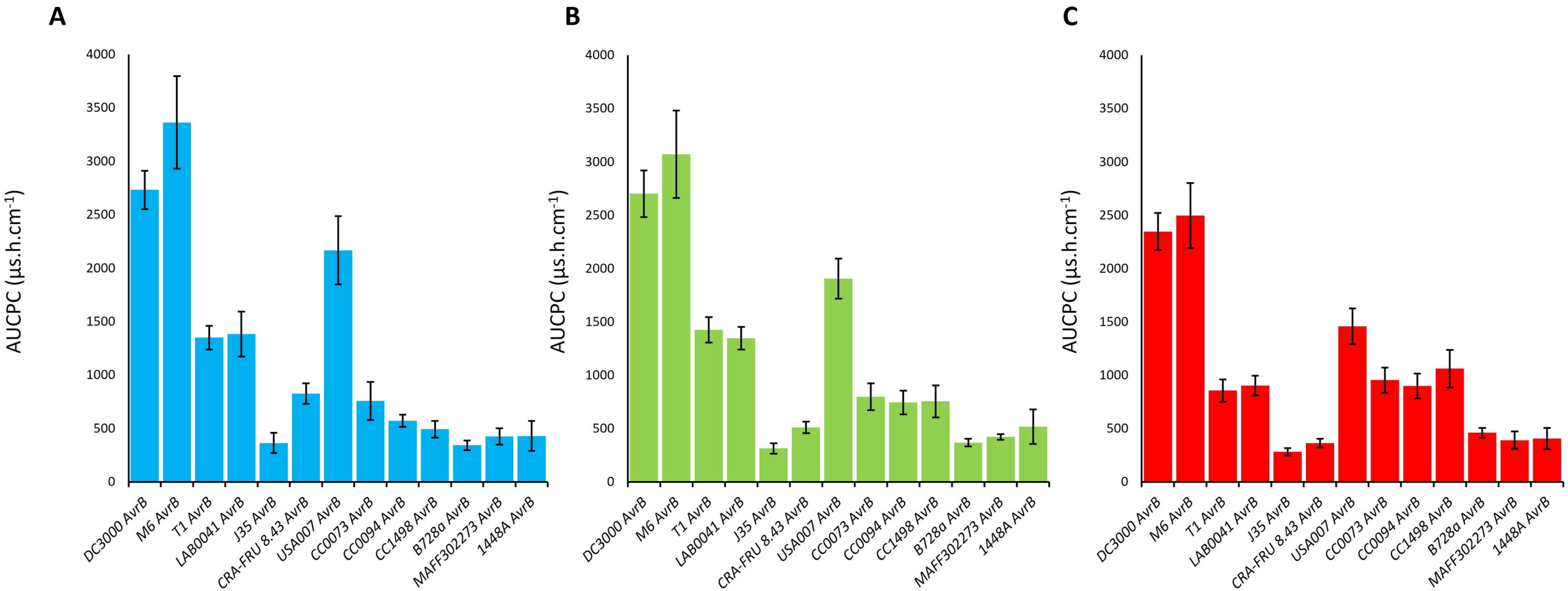
A
B
C
AUCPC (µs.h.cm-1)
4000
3500
3000
2500
2000
1500
1000
500
0
DC3000 AvrB
M6 AvrB
T1 AvrB
LAB0041 AvrB
J35 AvrB
CRA-FRU 8.43 AvrB
USA007 AvrB
CC0073 AvrB
CC0094 AvrB
CC1498 AvrB
B728a AvrB
MAFF302273 AvrB
1448A AvrB

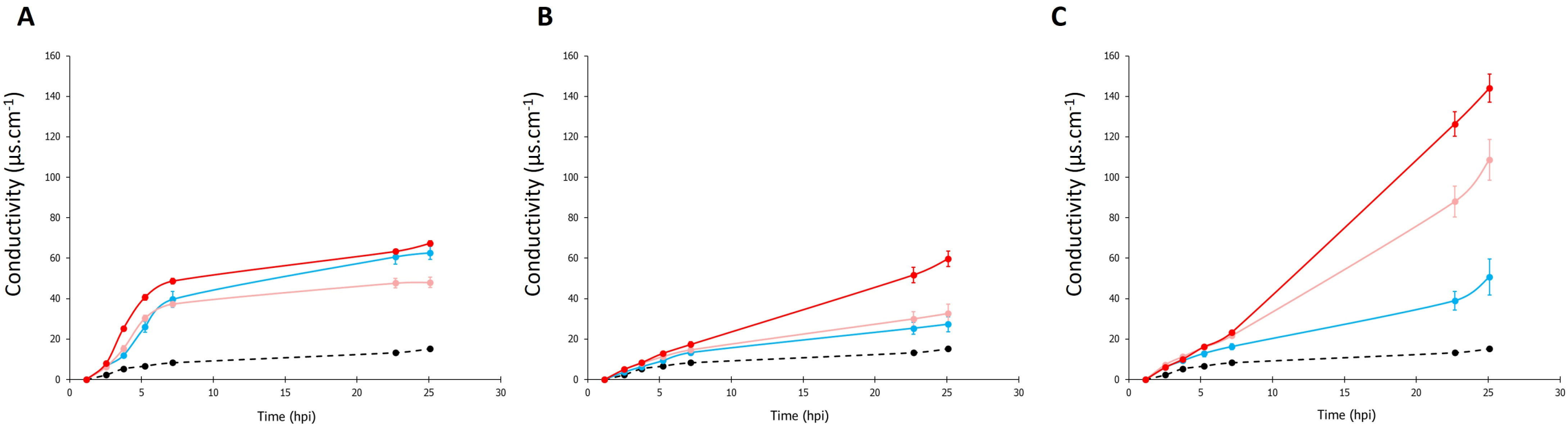
A
B
C
Conductivity (µs.cm-1)
Time (hpi)
0
20
40
60
80
100
120
140
160
0
5
10
15
20
25
30

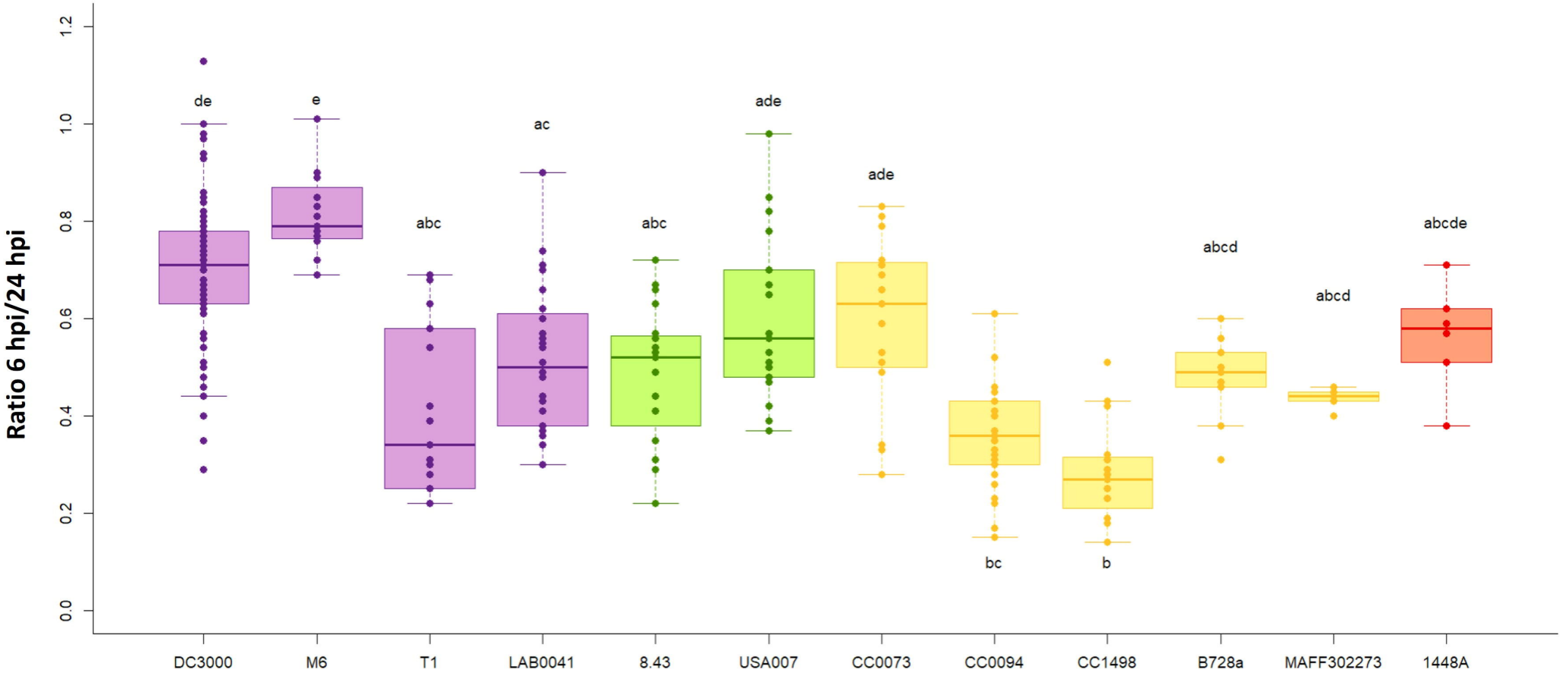
Ratio 6 hpi/24 hpi
0.0
0.2
0.4
0.6
0.8
1.0
1.2
de
e
abc
ac
abc
ade
ade
bc
b
abcd
abcd
abcde
DC3000
M6
T1
LAB0041
8.43
USA007
CC0073
CC0094
CC1498
B728a
MAFF302273
1448A

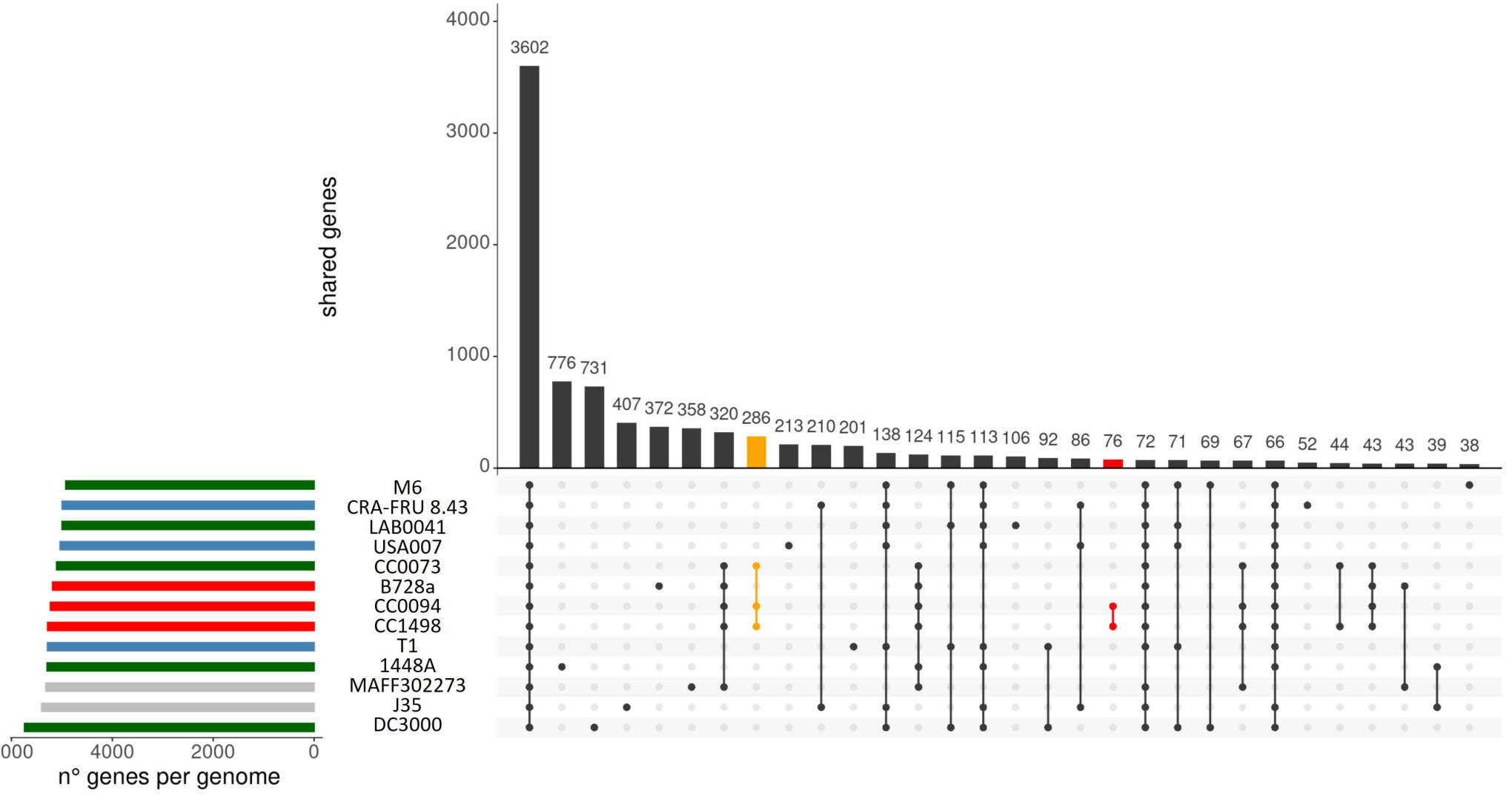
shared genes
4000
3000
2000
1000
0
3602
776
731
407
372
358
320
286
213
210
201
138
124
115
113
106
92
86
76
72
71
69
67
66
52
44
43
43
39
38
M6
CRA-FRU 8.43
LAB0041
USA007
CC0073
B728a
CC0094
CC1498
T1
1448A
MAFF302273
J35
DC3000
000
4000
2000
0
n° genes per genome